Research Square

Preprints are preliminary reports that have not undergone peer review.
They should not be considered conclusive, used to inform clinical practice,
or referenced by the media as validated information.

Geological controls on snowmelt runoff in a snowfall-dominated region of northern Japan: Implications for water resources management using decentralized water supply systems

Yohei Arata

arata-youhei@hro.or.jp

Hokkaido Research Organization https://orcid.org/0000-0002-7549-9227

Akiko NAGASAKA

Hokkaido Research Organization

Yu NAGASAKA

Hokkaido Research Organization

Ken USHIJIMA

Hokkaido Research Organization

Takanori KONO

Tottori University

Nobuo ISHIYAMA

Hokkaido University

Research Article

Keywords:

Posted Date: November 11th, 2026

DOI: https://doi.org/10.21203/rs.3.rs-10493715/v1

License: This work is licensed under a Creative Commons Attribution 4.0 International License.
Read Full License

Water Resources Management

Geological controls on snowmelt runoff in a snowfall-dominated region of northern Japan: Implications for water resources management using decentralized water supply systems

--Manuscript Draft--

Manuscript Number:	WARM-D-26-02554
Full Title:	Geological controls on snowmelt runoff in a snowfall-dominated region of northern Japan: Implications for water resources management using decentralized water supply systems
Article Type:	General paper
Keywords:	Volcanic geology; Geology-climate interactions; Multi-site observations; Spatial distribution of controlling factors; Mountainous rural regions; Sorachi River Basin
Abstract:	Mountainous rural regions are facing population decline and aging water infrastructure, increasing the need for decentralized water supply systems. Implementing these systems requires identifying watersheds suitable as water sources and their spatial distribution. In snowfall-dominated regions, where snowmelt runoff constitutes a major seasonal water resource, understanding the controls on snowmelt runoff is essential for identifying such watersheds. Although geological setting is often a primary control on runoff and therefore a key factor in identifying such watersheds, its influence on snowmelt runoff and its interactions with climatic conditions remain poorly understood. We evaluated the controls of climate, watershed geology, and their interactions on quick and delayed discharge during the snowmelt period across 33 forested watersheds (2.1–21.9 km2) in the Sorachi River basin, Hokkaido, northern Japan, using 153 watershed-year observations. Linear mixed models revealed that watershed geology exerted the strongest control on delayed discharge. In particular, delayed discharge increased with volcanic rock proportion, which also interacted significantly with snowfall water equivalent, indicating stronger geological effects under high-snowfall conditions. In contrast, quick discharge was controlled primarily by climatic conditions. Although volcanic rock proportion proved to be an effective indicator for identifying suitable source watersheds, watersheds with high volcanic rock proportions were concentrated in the eastern basin. In contrast, high-relief watersheds, the second most important control on delayed discharge, occurred mainly in the central and western parts of the basin, where non-volcanic geology predominates. Considering these complementary spatial patterns provides an important framework for decentralized water supply systems in mountainous rural regions.

Powered by Editorial Manager® and ProduXion Manager® from Aries Systems Corporation

Manuscript Click here to access/download;Manuscript;Manuscript.docx

27 July 2026

Submission to Water Resources Management

Geological controls on snowmelt runoff in a snowfall-dominated region of northern Japan: Implications for water resources management using decentralized water supply systems

Yohei ARATA[1*], Akiko NAGASAKA[1], Yu NAGASAKA[2], Ken USHIJIMA[3], Takanori KONO[4], Nobuo ISHIYAMA[5]

[1] Forestry Research Institute, Hokkaido Research Organization, Bibai, Hokkaido 079-0198, Japan.

[2] Research Fellow, Forestry Research Institute, Hokkaido Research Organization, Bibai, Hokkaido 079-0198, Japan.

[3] Northern Regional Building Research Institute, Hokkaido Research Organization, Asahikawa, Hokkaido 078-8801, Japan.

[4] Department of Social Management Engineering, Graduate School of Engineering, Tottori University, 4-101, Koyama-Minami, Tottori 680-8550, Japan.

[5] Research Faculty of Agriculture, Hokkaido University, Sapporo, Hokkaido 060-8589, Japan

*Corresponding author: Yohei Arata (arata-youhei@hro.or.jp), ORCID (0000-0002-7549-9227)

Abstract

Mountainous rural regions are facing population decline and aging water infrastructure, increasing the need for decentralized water supply systems. Implementing these systems requires identifying watersheds suitable as water sources and their spatial distribution. In snowfall-dominated regions, where snowmelt runoff constitutes a major seasonal water resource, understanding the controls on snowmelt runoff is essential for identifying such watersheds. Although geological setting is often a primary control on runoff and therefore a key factor in identifying such watersheds, its influence on snowmelt runoff and its interactions with climatic conditions remain poorly understood. We evaluated the controls of climate, watershed geology, and their interactions on quick and delayed discharge during the snowmelt period across 33 forested watersheds (2.1–21.9 km^2) in the Sorachi River basin, Hokkaido, northern Japan, using 153 watershed-year observations. Linear mixed models revealed that watershed geology exerted the strongest control on delayed discharge. In particular, delayed discharge increased with volcanic rock proportion, which also interacted significantly with snowfall water equivalent, indicating stronger geological effects under high-snowfall conditions. In contrast, quick discharge was controlled primarily by climatic conditions. Although volcanic rock proportion proved to be an effective indicator for identifying suitable source watersheds, watersheds with high volcanic rock proportions were concentrated in the eastern basin. In contrast, high-relief watersheds, the second most important control on delayed discharge, occurred mainly in the central and western parts of the

basin, where non-volcanic geology predominates. Considering these complementary spatial patterns provides an important framework for decentralized water supply systems in mountainous rural regions.

Keywords

Volcanic geology; Geology–climate interactions; Multi-site observations; Spatial distribution of controlling factors; Mountainous rural regions; Sorachi River Basin

1. INTRODUCTION

The sustainability of conventional water infrastructure is increasingly threatened, making the consideration of alternative water sources indispensable in regions experiencing rapid population decline or frequent natural disasters. In Japan, the total population is projected to decrease by approximately 20% by 2050 relative to 2008, with nearly 20% of municipalities expected to retain less than half of their 2020 population. In contrast, the water supply coverage rate has remained above 90% since 1978, reaching 98% in 2023 (Ministry of Land, Infrastructure, Transport and Tourism 2025). As a result, population decline combined with aging facilities has substantially increased the costs of maintaining and renewing large-scale, centralized water distribution networks, rendering conventional water supply management increasingly unsustainable.

This challenge is particularly pronounced in mountainous rural regions of Japan, where a transition toward small-scale and decentralized water supply systems that utilize local water resources has been emphasized as an effective response to a shrinking population (Matsumoto et al. 2013; Itoh et al. 2022). In practice, Furano city in Hokkaido, northern Japan has implemented a water supply system that relies primarily on forest surface water and springs, supported by small-scale water infrastructure (Ushijima et al. 2018; Ushijima and Masuda 2022). In addition, Japan is highly prone to natural disasters such as landslides and flooding associated with earthquakes and heavy rainfall, making the securing of alternative water sources essential for maintaining domestic water supply during emergencies (Ohnishi

and Kuwata 2012; Vrba 2016; Inokoshi et al. 2024; Nojima and Kato 2024). Similar challenges have been reported worldwide, including in California, United States (McReynolds and Simmons 1995), China (Huang et al. 2016), and West Bengal, India (Dhaneshwar et al. 1985). To address these challenges, it is necessary not only to estimate the volume of available water resources within a region but also to predict and clearly identify the spatial distribution of those resources (Wagener et al. 2010 Gnann et al. 2020; Zheng et al. 2023).

River discharge is governed by multiple watershed attributes. Climatic factors such as rainfall, snowfall, and temperature determine water input and seasonal dynamics and are often identified as the dominant controls in large-sample hydrological studies conducted at national to global scales (e.g., Beck et al. 2015; Addor et al. 2018; Zheng et al. 2023; Eslami et al. 2025). However, river discharge can differ markedly even among neighboring watersheds or those within the same region, reflecting the complexity of internal watershed attributes (Farvolden 1963; Pfister et al. 2017; Price 2011). The internal attributes, including geology, topography, and land cover, regulate storage capacity, permeability, and flow pathways. For instance, topographic indices have been shown to influence river discharge through groundwater contributions associated with watershed areas (Asano and Uchida 2010) and relief height (Inokoshi et al. 2024), drainage efficiency governed by watershed slope (Hewlett and Hibbert 1967), and storage capacity related to elevation (Staudinger et al. 2017). Geological settings, including rock type and age, also control permeability, storage capacity, and flow

pathways within watersheds, thereby influencing river discharge (e.g., Tague and Grant 2004; Onda et al. 2006; Iwasaki et al. 2021). Land cover is another critical factor that regulates water input to and storage within watersheds. For instance, forests strongly affect watershed water storage and downstream discharge through interception and transpiration in both rainfall-dominated (Momiyama et al. 2021, 2023) and snowfall-dominated regions (Wei et al. 2022; Abe et al. 2023). Quantifying the relative contributions of these climatic and internal watershed attributes is essential for identifying the factors that predominantly sustain water availability and shape its spatial distribution.

Among internal watershed attributes, geological setting often exerts a first-order control on runoff responses by regulating permeability and storage capacity (Uchida et al. 2016; Pfister et al. 2017). In particular, highly permeable geological formations, such as volcanic rocks, can strongly influence flow regimes by promoting groundwater storage and sustained discharge. For instance, in a 0.25-km² permeable volcanic watershed in southern Mexico, Muñoz-Villers and McDonnell (2012) found that the contribution of pre-event water to storm runoff increased from 35% to 99% as watershed wetness increased, indicating dominant vertical infiltration and runoff generation from deeper volcanic layers. Tague and Grant (2004) showed that young volcanic watersheds in the Oregon Cascades sustain higher baseflow and slower recession than older lithologies. Similarly, Iwasaki et al. (2021) found that river discharge increased with watershed area in volcanic watersheds because highly permeable lava layers increased groundwater contributions to streamflow in downstream reaches in northern Japan. In

addition, permeable volcanic rocks may exert stronger hydrological influence under wetter climatic conditions (Carlier et al. 2018; Hokanson et al. 2019). The geology-climate interactions have been reported for thermal regimes, where volcanic geology can enhance groundwater inputs and create cold-water refugia (Ishiyama et al. 2023), but their role in controlling flow regimes remains unclear.

Although substantial progress has been made in identifying the factors that govern river discharge, the controls on river discharge in snow-dominated regions remain poorly understood. In these regions, river discharge during the snowmelt period is a key component of the annual flow regime, driven by rising spring air temperatures and providing an important water resource (Barnett et al. 2005; Hunsaker et al. 2012). Because snowmelt runoff persists over several months, river discharge is likely influenced not only by climatic conditions that determine snowmelt input to the watershed, such as air temperature and snowfall, but also by internal watershed attributes that regulate water storage and release, including geology and topography (Miller et al. 2020; Brooks et al. 2025). Quantifying the relative contributions of climatic factors, internal watershed attributes, and their interactions is therefore essential for identifying the dominant controls on river discharge in snow-dominated regions.

The objective of this study is to evaluate the relative importance of climatic and internal watershed attributes, with particular emphasis on geological setting and its interaction with climate gradients, in controlling river discharge during the snowmelt periods across multiple independent watersheds in the Sorachi River basin, Hokkaido, northern Japan. Based on these results, we examine the spatial

distribution of the primary controlling factors and discuss their implications for water availability and water resource management in decentralized water supply systems. The Sorachi River basin is a suitable region for this purpose because it combines snow-dominated hydrology, pronounced geological heterogeneity (Suzuki et al. 2022; Ishiyama et al. 2023), and is largely composed of mountainous rural areas where water demand is spatially distributed (Ushijima et al. 2018; Ushijima and Masuda 2022).

2. METHODOLOGY

2.1 Study region

This study was conducted in the Sorachi River basin (2,650 km²: 43°-44° N, 141°-143° E), a tributary of the Ishikari River, in central Hokkaido, northern Japan (Fig. 1a). The climate (1991-2020) is mostly classified as Dfb (cold, warm-summer) and as Dfc (cold, cold-summer) at high-elevation sites, based on the Köppen climate classification (Beck et al. 2023). Mean annual precipitation and temperature at the approximate center of the study region are 1040 mm and 7.0 °C, respectively (1996-2025; AMeDAS Furano, Japan Meteorological Agency). Snow cover typically extends from November to May, and snowmelt mainly begins from late March to early April, resulting in snowmelt runoff. The Sorachi River basin is characterized by high-relief topography surrounded by mountainous terrain (Fig. 1b). An isolated peak, Mt. Irumukeppu (864.1 m), is situated in the northwestern part of

the basin, while Mt. Tokachi (2077.0 m) and Mt. Furano (1911.8 m), extending from the Taisetsu Mountain Range in a northeast-southwest direction, are located to the east. In the central part of the basin, Mt. Ashibetsu (1725.9 m) and Mt. Yubari (1667.6 m) extend in a north–south direction, and the southeastern part of the basin corresponds to the northernmost section of the Hidaka Mountain Range, which reaches elevations of up to 2052.1 m. Residential areas are concentrated along the valley of the Sorachi River that runs through these mountainous regions, while paddy fields and upland croplands are distributed in the surrounding valley bottoms and hilly areas (Fig. 1c). The upper part of the basin is predominantly covered by deciduous broadleaf forests, with some areas occupied by evergreen coniferous forests dominated by *Abies sachalinensis* and deciduous coniferous forests dominated by *Larix kaempferi*.

The underlying geology consists of accretionary complexes, sedimentary rocks, metamorphic rocks, plutonic rocks, and volcanic rocks (Fig. 1d). Volcanic rocks were broadly classified into three groups based on age and lithology: (i) young volcanic rocks (< 1.7 Ma), dominated by Pleistocene to Holocene non-alkaline mafic lavas and pyroclastic flows; (ii) old volcanic rocks (> 1.7 Ma), consisting of more consolidated volcanic rocks and pyroclastic deposits of Late Miocene to Pliocene age; and (iii) mixed volcanic debris of Late Miocene to Holocene age, characterized by high lithological heterogeneity. Volcanic rocks are distributed mainly in the eastern and northwestern parts of the region and originate from pyroclastic flow deposits of the Tokachi volcanic group (relatively young) and Mt.

Irumukeppu (relatively old), respectively.

The Sorachi River Basin contains water supply systems of various scales, ranging from individual household systems to large-scale systems serving more than 10,000 people, utilizing both groundwater and surface water. Two large dams (Kiyosato Dam and Kanayama Dam) have been constructed on the river for agricultural use within the basin and for domestic use in downstream areas outside the basin (Hokkaido Regional Development Bureau, Sapporo Development and Construction Department). Nevertheless, the largest water supply system in Furano City, the principal urban center in the basin, relies primarily on abundant groundwater resources (Furano City Water Supply Vision 2020–2029). Furthermore, in this city, community-managed decentralized water supply systems have also been implemented in suburban areas not covered by public water supply systems serving more than 100 people (Ushijima and Masuda 2022). These systems use spring water, surface water from forested watersheds, and groundwater from deep wells. As water supply pipelines continue to age and population decline progresses, both maintaining existing infrastructure and securing alternative water sources have become major challenges in the basin (2020–2029 Furano City Water Supply Vision; Ushijima 2025). In addition, this region may be increasingly affected by rain-on-snow events that trigger snowmelt-related hazards, including flooding and landslides (Ishi 2019), potentially damaging water infrastructure. Under these conditions, securing alternative water sources for emergency use has become increasingly important (Inokoshi et al. 2024).

2.2 Monitored watersheds and streamflow time-series data

Evaluating volcanic rocks as dominant controlling water discharge during snowmelt period was designed in multiple upstream watersheds within the Sorachi River basin (Fig. 1b-d). Thirty-three independent low-order forested watersheds (2.1-21.9 km²) were selected, spanning a 0-100% gradient in the proportion of volcanic rocks within each watershed (Fig. 1d; Table 1, also see Ishiyama et al. 2023). Mean watershed elevation ranged from 340 to 870 m, and mean channel gradients varied between 6° and 22° (GSI: Geospatial Information Authority of Japan). Channel morphology at watershed outlet was mostly classified as upstream channel types, including cascade, step-pool, and plane-bed reaches (Montgomery and Buffington 1997). The watersheds were forested, with a mean cover of 92.8% (range: 65-100%); evergreen forests accounted for 1-46% of the forested area, with the remainder composed of deciduous forests (JAXA: Japan Aerospace Exploration Agency). The dominant soil types are Brown Forest soils and non-allophanic and allophanic Andisols (NARO: National Agriculture and Food Research Organization).

To quantify snowmelt runoff characteristics, continuous discharge data were collected at the outlets of each watershed over multiple years. This multi-year dataset enabled analysis of discharge responses to varying meteorological conditions within the same watershed. Discharge was estimated by continuously measuring water depth with an absolute-pressure water-level sensor (U20L-04; HOBO)

and converting the recorded water depths to discharge using Manning's equation (see Fig. S1; Table S1; Text S1). Based on the streamflow time-series data, annual runoff and the runoff ratio to annual precipitation were calculated to assess data validity (Text S2). These indices were calculated only for years with discharge records available for more than 95% of the days.

2.3 Hydrograph separation into quick and delayed discharge

Characteristics of water discharge during the snowmelt period were evaluated by separating total discharge into two components: quick discharge (Q_q) and delayed discharge (Q_d) (Fig. 2). In this study, Q_q is interpreted as the rapidly responding runoff component, whereas Q_d represents the more slowly responding runoff component during the snowmelt period. These components are expected to reflect contrasting dominant flow pathways, with Q_q primarily associated with near-surface flow and Q_d with groundwater contributions from intermediate to deep subsurface storage. Following hydrograph separation methods originally developed for stormflow analysis (e.g., Tallaksen 1995; Gonzales et al. 2009), we applied a simple graphical method in which Q_q and Q_d were separated by a straight line connecting the onset and the end of the snowmelt runoff period. The end of the snowmelt runoff was defined as the second inflection point on the recession limb of the hydrograph, which is assumed to reflect the transition to delayed, groundwater-dominated discharge (Fukushima 1992; Tallaksen 1995). The first inflection point is assumed to represent the transition from rapid surface or near-surface flow

to shallow subsurface flow. To identify the two inflection points, changes in the slope of the recession limb were examined by approximating the hydrograph on a semi-logarithmic scale with a series of linear segments, each representing a period dominated by a different runoff component (Klaassen and Pilgrim 1975). Our hydrographs during the snowmelt season often exhibited repeated discharge increases during the recession phase because the snowmelt runoff period extends over several months. In such cases, an inflection point was defined as the point where the recession slope after an increase became gentler than the preceding recession slope. This procedure was repeated until the second inflection point was identified. Portions of the total discharge hydrograph located above the separation line were classified as Q_q, whereas portions below the line were classified as Q_d. This graphical separation method enables a consistent evaluation of snowmelt runoff characteristics over the entire snowmelt runoff period, including the rising limb, peak discharge, and recession limb of the hydrograph.

2.4. Covariates potentially influencing the snowmelt runoff components

Nine covariates as potential controls, including three climatic, one geologic, four topographic, and one land-cover variables, on snowmelt runoff were selected for identifying factors influencing quick discharge (Q_q) and delayed discharge (Q_d). The three climatic variables were gross precipitation as snowfall from October to March (hereafter snowfall water equivalent), gross precipitation from April

to May (spring precipitation), and the sum of positive daily mean air temperatures from February to May (degree-days). Snowfall water equivalent and spring precipitation were treated as inputs of water to the watersheds, whereas degree-days represented the potential intensity of snowmelt (Hock 2003). The geologic variable was the proportion of volcanic rock within each watershed. The four topographic variables were relief height, drainage density, average channel gradient, and the proportion of north-facing slopes. Among these, relief height was represented as an indicator influencing flow regime (Fennessey and Vogel 1990), drainage density and average channel gradient were represented as indicators of watershed drainage efficiency (Price 2011), and the proportion of north-facing slope was represented as an indicator reflecting snowmelt intensity due to solar radiation conditions (Miller et al. 2020). The land-cover variable was the proportion of evergreen forest cover, reflecting its influence on snow accumulation and snowmelt characteristics (Fujihara et al. 2017).

All covariates were derived from open-source spatial-information datasets. Climatic variables were obtained from the Agro-Meteorological Grid Square Data provided by the National Agriculture and Food Research Organization (Ohno et al. 2016; Kominami and Yamaguchi 2025). This dataset provides meteorological variables at a 1-km spatial resolution, including daily snowfall water equivalent (Code: SFW), daily precipitation (APCP), and daily mean air temperature (TMP_mea). The Sorachi River basin was divided into 1-km grid cells, and daily meteorological data were extracted at the centroids of all grid cells located within each monitored watershed. For each day, a watershed-

mean time series was computed by averaging the grid-cell values within the watershed. The climatic indices were then calculated from this watershed-mean time series. The geologic variable was derived from the 1:200,000 Seamless Geological Map of Japan (GeomapNAVI) provided by Geological Survey of Japan, the National Institute of Advanced Industrial Science and Technology. The proportion of volcanic rock within each watershed was calculated as total area fraction of young, old, and mixed volcanic rocks as well as volcanic debris. Topographic variables were derived from the 10-m resolution Digital Elevation Model provided by the Geospatial Information Authority of Japan. Relief height was calculated as the difference between the maximum and minimum elevations within each watershed. Mean channel gradient and drainage density were calculated from river networks delineated using the ArcHydro tool (ESRI) with a flow accumulation threshold of 200,000 m^2. Mean channel gradient was calculated as the average slope of grid cells intersected by the river network, and drainage density was calculated as the total channel length divided by watershed area. The proportion of north-facing slopes was calculated as the total area fraction of slopes oriented from northwest to northeast. Land-cover information was obtained from the 10-m resolution High-Resolution Land Use and Land Cover Map between 2018 and 2020 (v21.11) provided by Japan Aerospace Exploration Agency. All spatial analyses were conducted using ArcGIS Pro version 3.1.0 (ESRI).

2.5 Assessing the relative importance of factors controlling snowmelt runoff components

Linear mixed model (LMM) analysis was employed to quantitatively evaluate the relative importance of factors influencing both quick discharge (Q_q) and delayed discharge (Q_d). The dataset comprised 153 samples of Q_q and Q_d derived from 1-7 years of observations across 33 watersheds. For model construction, Q_q and Q_d were log-transformed to reduce the influence of large differences in magnitude among watersheds and were then used as response variables in the models. To compare their influential factors, both models used a consistent set of covariates, comprising the nine variables described above and two geologic-climatic interactions. Two interactions, volcanic rock × snowfall water equivalent and volcanic rock × spring precipitation, were included to examine geological effects along climatic gradients. All covariates were standardized prior to analysis to avoid scale-related biases. No strong correlations were detected among the covariates (Fig. S2), and variance inflation factors ranged from 1.0 to 2.0, indicating a low risk of multicollinearity (VIF < 10; Neter et al. 1996). Because snowmelt runoff was observed repeatedly within the same watersheds, watershed identity was included as a random intercept to account for non-independence among observations and unmeasured watershed-specific characteristics. Interannual variability was explicitly represented by year-specific climatic covariates.

Models were then evaluated through model comparison, statistical significance and relative importance of covariates, and overall model performance. Model selection was conducted using the Akaike information criterion corrected for small sample size (AICc) (Akaike 1998), and model

averaging for superior models was applied to candidate models with ΔAICc < 2. The significance of each covariate was assessed using 95% confidence intervals of parameter estimates in the averaged model, with covariates whose confidence intervals did not include zero identified as influential factors. The relative importance of selected covariates was evaluated using the absolute values of standardized coefficients. Model performance was assessed using marginal R^2, representing variance explained by covariates alone, conditional R^2, representing variance explained by both covariates and random effects, and the root mean square error of model residuals (RMSE: Moriasi et al. 2007). These evaluation procedures of constructed models allow us to develop strong reliable models. All statistical analyses were conducted using R ver. 4.5.2 (R Core Team 2025).

3. RESULTS

3.1 Snowmelt runoff characteristics among watersheds

Estimated water discharge during 2018–2024, derived from in-situ water-level observations, varied considerably among watersheds. Mean manning's roughness coefficients ranged from 0.06 to 0.69, with a mean of 0.19 (Table S1). Based on these coefficients, mean annual runoff ranged from 420 to 2680 mm, with a mean of 1060 mm (Table S2). Annual runoff ratios to annual precipitation ranged from 0.29 to 2.32, with a mean of 0.84. High mean runoff ratios (>1) were observed in watersheds Nos. 5, 7, 11, 13, 23, and 27 (Table S2).

Hydrographs averaged across all watersheds exhibited a common seasonal pattern characterized by distinct snowmelt runoff (Fig. S3). Runoff increased markedly in response to rapid decreases in snow depth during the snowmelt period (typically March–April), forming pronounced peaks before gradually declining toward summer (approximately July). During this recession period and the subsequent snow-free season, runoff was characterized primarily by short-term increases associated with rainfall events. Temporary runoff increases during the snowmelt period were also observed in 2018 and 2020 in association with rain-on-snow events (Fig. S3). Years with greater snow accumulation and concentrated snowmelt exhibited larger spring runoff peaks (e.g., 2018 and 2023), whereas years with lower snow accumulation or more gradual snowmelt produced relatively smaller peaks (e.g., 2019 and 2020) (Fig. S3).

Although all watersheds exhibited similar seasonal runoff patterns, the magnitudes of their snowmelt runoff components differed substantially. For each watershed, the multi-year mean quick discharge (Q_q) ranged from 58 to 412 mm, whereas the multi-year mean delayed discharge (Q_d) ranged from 33 to 366 mm (Table S2). Although neither runoff component showed a clear or consistent relationship with snowfall water equivalent or spring precipitation, Q_q tended to increase in watersheds with greater snowfall water equivalent and spring precipitation, suggesting that water supply during the snowmelt period partly influences this runoff component (Fig. S4). In contrast, Q_d varied widely regardless of these meteorological conditions, indicating little sensitivity to climatic variation (Fig.

S4). These results suggest that Q_q is more responsive to meteorological conditions, whereas Q_d is likely governed primarily by non-meteorological factors, such as internal watershed attributes.

3.2 Identification of factors influencing quick and delayed discharge and their relative importance

Quick discharge (Q_q) was influenced by three variables, as indicated by model averaging of nine superior candidate models (ΔAICc < 2), with standardized coefficients showing that variables related to meteorological factors exerted relatively stronger effects than internal watershed attributes (Table S3). The best model showed the variation in Q_q with a marginal R^2 of 0.40, a conditional R^2 of 0.76, and an RMSE of 0.13 (Fig. S5a; Table S4), indicating good performance in reproducing the observed variability in Q_q. In the averaged model, the most influential factor was spring precipitation (standardized coefficient = 0.102), followed by average channel gradient (0.088) and snowfall water equivalent (0.065) (Fig. 3a; Table 2). Q_q increased with increasing spring precipitation, average channel gradient, and snowfall water equivalent (Fig. S6a-c). With the exception of average channel gradient, internal watershed attributes including volcanic rock proportion, relief, and drainage density did not significantly affect Q_q.

Delayed discharge (Q_d) was influenced by three variables and one interaction identified through model averaging of nine superior models (ΔAICc < 2) (Table S3). In contrast to quick discharge, standardized coefficients indicated that internal watershed attributes were relatively more influential

than meteorological factors. The best model reproduced the variation in Q_d with a marginal R^2 of 0.53, a conditional R^2 of 0.74, and an RMSE of 0.14 (Fig. S5b; Table S4), demonstrating good model performance. In the averaged model, Q_d was significantly and positively influenced by proportion of volcanic rock, watershed relief, and spring precipitation; the proportion of volcanic rock within watersheds was the most influential factor (standardized coefficient = 0.140), followed by watershed relief (0.133) and spring precipitation (0.061) (Fig. 3b; Table 2; Fig. S6d-f). The interaction between volcanic rock proportion and snowfall water equivalent significantly affected Q_d, indicating that the effect of volcanic rock proportion on Q_d depended on snowfall conditions (Fig. 3b). Under low snowfall water equivalent conditions, log (Q_d) remained low regardless of volcanic rock proportion, whereas under higher snowfall water equivalent conditions, log (Q_d) increased markedly with increasing volcanic rock proportion (Fig. 4). This pattern indicates that large, delayed discharge preferentially occurred when both volcanic rock proportion and snowfall water equivalent were high, reflecting a nonlinear combined influence of these two factors on Q_d.

4. DISCUSSION

4.1 Validity of estimated water discharge

The water discharge estimated in this study based on Manning's equation appears reasonable, as both the adopted roughness coefficients and the resulting runoff characteristics were generally

consistent with previous studies. The Manning's roughness coefficients (0.06–0.69, mean 0.19) were within the range reported for mountain streams. For instance, Asano et al. (2012) reported coefficients of 0.14–1.88 for a step–pool channel (drainage area: 0.09 km²) in central Japan, while, based on observations in Colorado, David et al. (2010) estimated values ranging from 0.09–0.23 (minimum) to 0.18–0.40 (maximum) across multiple sites (0.69–8.73 km²).

The resulting discharge estimates also reproduced hydrological characteristics expected for the study region. The hydrographs captured the distinct spring snowmelt runoff typical of the Sorachi River basin, and annual runoff ratios (0.29–0.95 for most watersheds) were generally comparable to those reported by Oda et al. (2024) for Japanese watersheds (1–24 km²; 0.39–0.88). Runoff ratios exceeded 1 in six watersheds (Nos. 5, 7, 11, 13, 23, and 27), with values exceeding unity potentially arising from a combination of uncertainties in watershed water balance estimates and hydrological complexities, such as groundwater exchanges across topographic watershed boundaries (Masaoka et al. 2021). The six watersheds with runoff ratios exceeding 1 are either dominated by volcanic rocks or comprise multiple geological units, which may result in complex subsurface hydrogeological structures. Taken together, these findings support the validity of the estimated discharge and its use for evaluating controls on snowmelt runoff among watersheds.

4.2 Geological effects on snowmelt runoff components

Geological effects on runoff components were particularly evident for delayed discharge, whereas no statistically significant influence on quick discharge was detected in the LMM analysis. A comparison of hydrographs between volcanic watersheds (>90%) and non-volcanic watersheds (<10%) exhibited higher baseflow and a slower recession in the former (Fig. S7), suggesting greater groundwater contributions. Similar hydrograph characteristics have been reported for young volcanic watersheds in the Oregon Cascade Range, USA (Tague and Grant 2004). The finding that volcanic watersheds sustain larger delayed discharge is consistent with previous studies conducted in the same region, which inferred strong groundwater contributions based on the clear cooling effect on summer stream temperature in volcanic watersheds (Ishiyama et al. 2023; Suzuki et al. 2022). In the study area, relatively young volcanic deposits (particularly around Mt. Furano and Mt. Tokachi) may provide large subsurface storage due to unconsolidated bedrock (Tague and Grant 2004; Muñoz-Villers and McDonnell 2012; Iwasaki et al. 2021).

The positive interaction between volcanic rock proportion and snowfall water equivalent further underscores the complex effect of volcanic rock. Under low-snowfall conditions, water input may be insufficient to activate the large subsurface storage capacity of permeable volcanic formations, resulting in limited delayed discharge even in volcanic watersheds. By contrast, under high-snowfall conditions, sustained meltwater input can infiltrate into volcanic layers, be temporarily stored, and substantially released as delayed discharge. Thus, the interaction between underlying geology and

climate can be interpreted as a supply-dependent storage effect in snowy regions. This climate-dependent geological effect is consistent with previous findings that volcanic geology interacts with climatic conditions to shape stream environments (Ishiyama et al. 2023), although the present study highlights this interaction through snowmelt storage and delayed runoff rather than summer thermal regimes.

In addition to geology, relief height was identified as a secondary control, further underscoring importance of subsurface water dynamics in delayed discharge. Increasing elevation differences promote subsurface flow along bedding planes and bedrock fractures, thereby enhancing groundwater contributions, as reported in sedimentary rock watersheds (e.g., Onda et al. 2006; Inokoshi et al. 2024). In this study area, sedimentary rocks are widely distributed from the western to central regions, particularly around Mt. Ashibetsu to Mt. Yubari, where steep terrain and large elevation differences likely promote strong groundwater contributions. Indeed, delayed discharge is relatively high in watersheds located in these areas (see Figs. 1 and S4).

Quick discharge, for which geological effects were not statistically significant, was primarily governed by climatic factors (i.e., snowfall water equivalent and spring precipitation), indicating stronger sensitivity to external water inputs than to internal watershed attributes. The finding that spring precipitation (April–May) was a more influential variable than snowfall water equivalent suggests that additional water inputs during the snowmelt season can enhance subsurface storage and

activate lateral and shallow subsurface flow pathways (McGuire and McDonnell 2010; Asano and Uchida 2018), thereby prolonging the duration of snowmelt runoff and contributing to increased quick discharge. In particular, the involvement of the "rain-on-snow" phenomenon may also contribute to enhanced quick discharge (e.g., 2018 and 2021 events in Fig. S3). Rainwater may move rapidly through an already wet soil matrix during snowmelt periods, delivering a concentrated pulse of water to the stream over a short period and thereby triggering a pronounced quick discharge response (Brandt et al. 2022). In addition to climatic factors, the positive correlation with mean channel slope reflects the physical characteristic where steeper channels efficiently transport supplied water downstream (Hewlett and Hibbert 1967). These results suggest that quick discharge is controlled mainly by short-term hydrometeorological forcing and drainage efficiency within the watershed.

4.3 Implications for water resources management using decentralized water supply systems

Decentralized water supply systems require not only the identification of key watershed attributes that enable a stable water supply but also consideration of their spatial arrangement. Because delayed discharge was more strongly controlled by internal watershed attributes and sustained discharge than quick discharge, we mapped the spatial distribution of the key watershed attributes controlling delayed discharge across the Sorachi River basin. Volcanic rock proportion, the first-order control on delayed discharge, and relief height, the second-order control, were mapped using the Watershed tool in

ArcGIS Pro version 3.1.0 (Fig. 5). A minimum drainage area of 1 km^2 was adopted to delineate watersheds of a size that could realistically function as local water sources while excluding very small headwater watersheds. The resulting maps show that watersheds with high proportions of volcanic rock are concentrated around Mt. Furano and Mt. Tokachi (Fig. 5a), whereas watersheds with relatively high relief are distributed mainly across the central and western parts of the basin (Fig. 5b). These results indicate that the key watershed attributes controlling delayed discharge exhibit distinct spatial distributions across the basin.

The uneven spatial distribution of watersheds with high proportions of volcanic rock indicates that, although volcanic rock has the greatest potential to provide stable water resources, relying solely on volcanic watersheds is unlikely to support water supply across all rural communities where decentralized water supply systems are required within the basin. In contrast, relief height, the second most important watershed attribute controlling delayed discharge, identifies additional watersheds with high potential in the non-volcanic regions along the Ashibetsu foothills, where sedimentary rocks predominate, thereby complementing areas with low volcanic rock proportions. These results suggest that volcanic and non-volcanic watersheds make complementary contributions to regional water resources through different watershed characteristics controlling delayed discharge. Moreover, because the influence of volcanic rock on delayed discharge depends on snowfall water equivalent, its effectiveness may decline if snow accumulation decreases under future climatic conditions, further

emphasizing the importance of complementary watershed attributes. Combining volcanic rock proportions with complementary watershed attributes, such as relief height, would therefore provide a more robust and climate-resilient framework for water resource management using decentralized water supply systems.

5. SUMMARY AND CONCLUSION

This study evaluated the relative importance of climatic factors, internal watershed attributes, and their interactions controlling snowmelt runoff components (quick and delayed discharge) using multi-site discharge observations and linear mixed models across 33 independent snowfall-dominated, forested watersheds in the Sorachi River watershed, Hokkaido, Japan. The main findings are as follows: (1) quick discharge is strongly governed by external climatic inputs such as spring precipitation and snowfall water equivalent, whereas delayed discharge is more strongly influenced by internal watershed attributes, including geology (proportion of volcanic rock) and topography (relief height); and (2) in volcanic watersheds, delayed discharge is sustained by enhanced groundwater contributions, and the storage capacity associated with volcanic rock becomes more pronounced under conditions of higher snowfall water equivalent, indicating an interaction between geological and climatic controls. These results highlight the importance of developing predictive models that capture the characteristics of each runoff component. Furthermore, analysis of the spatial

arrangements of controlling factors revealed that volcanic rock, the primary control on delayed discharge, is unevenly distributed within the region, indicating that water source evaluation incorporating secondary factors is important for selecting water sources and identifying appropriate intake locations. Overall, the findings of this study provide a fundamental framework for water resources management using decentralized water supply systems in mountainous rural regions facing population decline and aging water infrastructure.

6. REFERENCES

Abe T, Kubota T, Noguchi S, Hosoda I (2023) Effects of clear-cutting and forest regrowth on snowmelt runoff in the Kamabuchi experimental watershed in northern Japan. J Jpn For Soc 105:1–10. (in Japanese with English abstract). https://doi.org/10.4005/jjfs.105.1

Addor N, Nearing G, Prieto C, et al (2018) A Ranking of Hydrological Signatures Based on Their Predictability in Space. Water Resources Research 54:8792–8812. https://doi.org/10.1029/2018WR022606

Akaike H (1998) Information theory and an extension of the maximum likelihood principle. In: Parzen E, Tanabe K, Kitagawa G (eds) Selected Papers of Hirotugu Akaike. Springer Series in Statistics. Springer, New York, NY, pp 199–213. https://doi.org/10.1007/978-1-4612-1694-0_15

Asano Y, Hoshino S, Uchida T, Akiyama K (2012) Measuring the flow and Manning's roughness coefficient of mountain streams. J Jpn Soc Eros Control Eng 65:62–68. (in Japanese with English abstract). https://doi.org/10.11475/sabo.65.1_62

Asano Y, Uchida T (2010) Is representative elementary area defined by a simple mixing of variable small streams in headwater catchments? Hydrological Processes 24:666–671. https://doi.org/10.1002/hyp.7589

Asano Y, Uchida T (2018) The roles of channels and hillslopes in rainfall/run-off lag times during intense storms in a steep catchment. Hydrological Processes 32:713–728. https://doi.org/10.1002/hyp.11443

Barnett TP, Adam JC, Lettenmaier DP (2005) Potential impacts of a warming climate on water availability in snow-dominated regions. Nature 438:303–309. https://doi.org/10.1038/nature04141

Beck HE, De Roo A, Van Dijk AIJM (2015) Global Maps of Streamflow Characteristics Based on Observations from Several Thousand Catchments*. Journal of Hydrometeorology 16:1478–1501. https://doi.org/10.1175/JHM-D-14-0155.1

Beck HE, McVicar TR, Vergopolan N, et al (2023) High-resolution (1 km) Köppen-Geiger maps for 1901–2099 based on constrained CMIP6 projections. Sci Data 10:724. https://doi.org/10.1038/s41597-023-02549-6

Brandt WT, Haleakala K, Hatchett BJ, Pan M (2022) A Review of the Hydrologic Response Mechanisms During Mountain Rain-on-Snow. Front Earth Sci 10:791760. https://doi.org/10.3389/feart.2022.791760

Brooks PD, Solomon DK, Kampf S, et al (2025) Groundwater dominates snowmelt runoff and controls streamflow efficiency in the western United States. Commun Earth Environ 6:341. https://doi.org/10.1038/s43247-025-02303-3

Carlier C, Wirth SB, Cochand F, et al (2018) Geology controls streamflow dynamics. Journal of Hydrology 566:756–769. https://doi.org/10.1016/j.jhydrol.2018.08.069

David GCL, Wohl E, Yochum SE, Bledsoe BP (2010) Controls on spatial variations in flow resistance

along steep mountain streams. Water Resources Research 46:2009WR008134. https://doi.org/10.1029/2009WR008134

Dhaneshwar RS, Basu AK, Biswas AK, Ganguly AK, Sanyal PB (1985) Evaluation of selected rural water supply schemes in West Bengal. In: Proceedings of the 11th WEDC Conference: Water and Waste Engineering for Developing Countries, pp 128–131.

Eslami Z, Seybold H, Kirchner JW (2025) Climatic, topographic, and groundwater controls on runoff response to precipitation: evidence from a large-sample data set. https://doi.org/10.5194/egusphere-2025-35

Farvolden RN (1963) Geologic controls on ground-water storage and base flow. J Hydrol 1:219–249. https://doi.org/10.1016/0022-1694(63)90004-0

Fennessey N, Vogel RM (1990) Regional Flow-Duration Curves for Ungauged Sites in Massachusetts. J Water Resour Plann Manage 116:530–549. https://doi.org/10.1061/(ASCE)0733-9496(1990)116:4(530)

Fujihara Y, Takase K, Chono S, Ichion E, Ogura A, Tanaka K (2017) Influence of topography and forest characteristics on snow distributions in a forested catchment. J Hydrol 546:289–298. https://doi.org/10.1016/j.jhydrol.2017.01.021

Fukushima Y (1992) Prediction of rainfall runoff in mountainous watersheds (in Japanese). In: Tsukamoto Y (ed) Forest Hydrology (in Japanese). Buneido Publishing, Tokyo, Japan, pp 171–194

Furano City (2021) Furano City Water Supply Vision (2020–2029). Furano City, Hokkaido, Japan. (in Japanese). https://www.city.furano.hokkaido.jp/fs/3/7/4/7/8/_/20210310_suidouvision.pdf

Gnann SJ, McMillan HK, Woods RA, Howden NJK (2021) Including regional knowledge improves baseflow signature predictions in large sample hydrology. Water Resour Res 57:e2020WR028354. https://doi.org/10.1029/2020WR028354

Gonzales AL, Nonner J, Heijkers J, Uhlenbrook S (2009) Comparison of different base flow separation methods in a lowland catchment. Hydrol Earth Syst Sci 13:2055–2068. https://doi.org/10.5194/hess-13-2055-2009

Hewlett JD, Hibbert AR (1967) Factors affecting the response of small watersheds to precipitation in humid areas. In: Sopper WE, Lull HW (eds) Forest Hydrology: Proceedings of a National Science Foundation Advanced Science Seminar. Pergamon Press, New York, pp 275–290.

Hock R (2003) Temperature index melt modelling in mountain areas. Journal of Hydrology 282:104–115. https://doi.org/10.1016/S0022-1694(03)00257-9

Hokanson KJ, Mendoza CA, Devito KJ (2019) Interactions Between Regional Climate, Surficial Geology, and Topography: Characterizing Shallow Groundwater Systems in Subhumid, Low-Relief Landscapes. Water Resources Research 55:284–297. https://doi.org/10.1029/2018WR023934

Huang J, Lou I, Li Y (2016) Integrated water resources management for emergency situations: A case

study of Macau. J Environ Sci 50:72–78. https://doi.org/10.1016/j.jes.2016.04.023

Hunsaker CT, Whitaker TW, Bales RC (2012) Snowmelt Runoff and Water Yield Along Elevation and Temperature Gradients in California's Southern Sierra Nevada1. J American Water Resour Assoc 48:667–678. https://doi.org/10.1111/j.1752-1688.2012.00641.x

Inokoshi S, Gomi T, Chiu CW, Onda Y, Asai K (2024) Baseflow distribution and geomorphic characteristics of headwaters for obtaining distributed domestic water sources during natural disasters. J Jpn Soc Hydrol Water Resour 37:335–350. (in Japanese with English abstract). https://doi.org/10.3178/jjshwr.37.1840

Ishii Y (2019) Snow hydrological impacts due to rain-on-snow events. Low Temp Sci 77:41–48. (in Japanese with English abstract). https://doi.org/10.14943/lowtemsci.77.41

Ishiyama N, Sueyoshi M, García Molinos J, et al (2023) Underlying geology and climate interactively shape climate change refugia in mountain streams. Ecological Monographs 93:e1566. https://doi.org/10.1002/ecm.1566

Itoh S, Nakanishi T, Zeng J (2022) How to supply safe drinking water in small water supply systems. J Natl Inst Public Health 71:225–233. (in Japanese with English abstract). https://doi.org/10.20683/jniph.71.3_225

Iwasaki K, Nagasaka Y, Nagasaka A (2021) Geological Effects on the Scaling Relationships of Groundwater Contributions in Forested Watersheds. Water Resources Research 57:e2021WR029641. https://doi.org/10.1029/2021WR029641

Klaassen BE, Pilgrim DH (1975) Hydrograph recession constants for New South Wales streams. Civ Eng Trans Inst Eng Aust 17:43–49.

Kominami Y, Yamaguchi T (2025) Snow cover data of the Agro-Meteorological Grid Square Data, NARO. Journal of Agricultural Meteorology.

Masaoka N, Kosugi K, Fujimoto M (2021) Bedrock Groundwater Catchment Area Unveils Rainfall-Runoff Processes in Headwater Basins. Water Resources Research 57:e2021WR029888. https://doi.org/10.1029/2021WR029888

Matsumoto K, Hoshino S, Yogo T (2013) Research on Sustaining Small-scale Water Supply Cooperatives in Communities. Journal of Rural Problems 49:82–88. https://doi.org/10.7310/arfe.49.82

McGuire KJ, McDonnell JJ (2010) Hydrological connectivity of hillslopes and streams: Characteristic time scales and nonlinearities. Water Resources Research 46:2010WR009341. https://doi.org/10.1029/2010WR009341

McReynolds L, Simmons RL (1995) LA's rehearsal for the big one. J Am Water Works Assoc 87:65–70. https://doi.org/10.1002/j.1551-8833.1995.tb06363.x

Miller SA, Lyon SW, Miller SN (2020) Quantifying contributions of snowmelt water to streamflow using graphical and chemical hydrograph separation. Hydrol Process 34:5606–5623.

https://doi.org/10.1002/hyp.13981

Ministry of Land, Infrastructure, Transport and Tourism (2025) Future directions for centralized and decentralized water and sewerage systems. Ministry of Land, Infrastructure, Transport and Tourism, Tokyo, Japan. (in Japanese). https://www.mlit.go.jp/mizukokudo/sewerage/content/001912069.pdf

Momiyama H, Kumagai T, Egusa T Model analysis of forest thinning impacts on the water resources during hydrological drought periods. Forest Ecology and Management 499:119593. https://doi.org/10.1016/j.foreco.2021.119593

Momiyama H, Kumagai T, Fujime N, et al (2023) Forest canopy interception can reduce flood discharge: Inferences from model assumption analysis. Journal of Hydrology 623:129843. https://doi.org/10.1016/j.jhydrol.2023.129843

Montgomery DR, Buffington JM (1997) Channel-reach morphology in mountain drainage basins. Geological Society of America Bulletin 109:596–611. https://doi.org/10.1130/0016-7606(1997)109%253C0596:CRMIMD%253E2.3.CO;2

Moriasi DN, Arnold JG, Van Liew MW, et al (2007) Model Evaluation Guidelines for Systematic Quantification of Accuracy in Watershed Simulations. Transactions of the ASABE 50:885–900. https://doi.org/10.13031/2013.23153

Muñoz-Villers LE, McDonnell JJ (2012) Runoff generation in a steep, tropical montane cloud forest catchment on permeable volcanic substrate. Water Resources Research 48:2011WR011316. https://doi.org/10.1029/2011WR011316

Oda T, Iwasaki K, Egusa T, et al (2024) Scale-Dependent Inter-Catchment Groundwater Flow in Forested Catchments: Analysis of Multi-Catchment Water Balance Observations in Japan. Water Resources Research 60:e2024WR037161. https://doi.org/10.1029/2024WR037161

Ohnishi Y, Kuwata Y (2012) A study on emergency water delivery in wide-area earthquake disaster: A case study of the Great East Japan Earthquake Disaster. J Jpn Soc Civ Eng Ser A1 (Struct Earthq Eng) 68:I_930–I_939. (in Japanese with English abstract). https://doi.org/10.2208/jscejseee.68.I_930

Ohno H, Sasaki K, Ohara G, Nakazono K (2016) Development of grid square air temperature and precipitation data compiled from observed, forecasted, and climatic normal data. Climate in Biosphere 16:71–79. https://doi.org/10.2480/cib.J-16-028

Onda Y, Tsujimura M, Fujihara J, Ito J (2006) Runoff generation mechanisms in high-relief mountainous watersheds with different underlying geology. Journal of Hydrology 331:659–673. https://doi.org/10.1016/j.jhydrol.2006.06.009

Pfister L, Martínez-Carreras N, Hissler C, et al (2017) Bedrock geology controls on catchment storage, mixing, and release: A comparative analysis of 16 nested catchments. Hydrological Processes 31:1828–1845. https://doi.org/10.1002/hyp.11134

Price K (2011) Effects of watershed topography, soils, land use, and climate on baseflow hydrology in humid regions: A review. Progress in Physical Geography: Earth and Environment 35:465–492. https://doi.org/10.1177/0309133311402714

R Core Team (2025) R: A language and environment for statistical computing. R Foundation for Statistical Computing, Vienna, Austria

Staudinger M, Stoelzle M, Seeger S, et al (2017) Catchment water storage variation with elevation. Hydrological Processes 31:2000–2015. https://doi.org/10.1002/hyp.11158

Suzuki H, Nakatsugawa M, Ishiyama N (2022) Climate Change Impacts on Stream Water Temperatures in a Snowy Cold Region According to Geological Conditions. Water 14:2166. https://doi.org/10.3390/w14142166

Tague C, Grant GE (2004) A geological framework for interpreting the low-flow regimes of Cascade streams, Willamette River Basin, Oregon. Water Resources Research 40:2003WR002629. https://doi.org/10.1029/2003WR002629

Tallaksen LM (1995) A review of baseflow recession analysis. J Hydrol 165:349–370. https://doi.org/10.1016/0022-1694(94)02540-R

Uchida T, Tomomura M, Sato Y, Asano Y, Kambara J (2016) An analysis for main controls of rainfall-runoff response function at mountainous headwater catchments through a comparative hydrological approach. Trans Jpn Geomorphol Union 37:579–595. (in Japanese with English abstract). https://doi.org/10.60380/tjgu.37.4_579

Ushijima K (2025) Community-based water supply system in Hokkaido, Japan. J Environ Conserv Eng 54:60–65. (in Japanese with English abstract). https://doi.org/10.5956/jriet.54.2_60

Ushijima K, Ishii A, Fukui J, Matsumura H (2018) Feasibility of community-based water management systems based on a field study in depopulated regions. J Jpn Soc Civ Eng Ser G (Environ Res) 74:III_143–III_152. (in Japanese with English abstract). https://doi.org/10.2208/jscejer.74.III_143

Ushijima K, Masuda T (2022) Community-based autonomous management of small water supply systems and practical approaches. J Natl Inst Public Health 71:254–263. (in Japanese with English abstract). https://doi.org/10.20683/jniph.71.3_254

Vrba J (2016) The role of groundwater governance in emergencies during different phases of natural disasters. Hydrogeol J 24:287–302. https://doi.org/10.1007/s10040-015-1353-z

Wagener T, Sivapalan M, Troch PA, et al (2010) The future of hydrology: An evolving science for a changing world. Water Resources Research 46:2009WR008906. https://doi.org/10.1029/2009WR008906

Wei X, Giles-Hansen K, Spencer SA, et al (2022) Forest harvesting and hydrology in boreal Forests: Under an increased and cumulative disturbance context. Forest Ecology and Management 522:120468. https://doi.org/10.1016/j.foreco.2022.120468

Zheng Y, Coxon G, Woods R, et al (2023) Controls on the Spatial and Temporal Patterns of Rainfall-

Runoff Event Characteristics—A Large Sample of Catchments Across Great Britain. Water Resources Research 59:e2022WR033226. https://doi.org/10.1029/2022WR033226

Acknowledgement

We sincerely thank the members of Forest Environment Division, Forestry Research Institute, Hokkaido Research Organization for their invaluable assistance with the field surveys.

Statements and Declarations

Funding This study was primarily supported by JSPS KAKENHI (Grant Number: 24K17927). Additional support was provided by a Priority Research Program of the Hokkaido Research Organization, JSPS KAKENHI (Grant Numbers: 23K25050 and 25H01191), and the research fund for the Ishikari and Tokachi Rivers provided by the Ministry of Land, Infrastructure, Transport and Tourism (MLIT) of Japan. This study was also supported by Scientific Research Grant for Water Supply and Sewerage (Grant Number: JPJ012969) and a Strategic Research Grant from the Hokkaido Research Organization.

Competing Interests The authors have no relevant financial or non-financial interests to disclose.

Author Contributions Yohei Arata, Akiko Nagasaka, Yu Nagasaka, and Nobuo Ishiyama contributed to the conception and design of the study. Material preparation and data collection were performed by Yohei Arata, Akiko Nagasaka, Yu Nagasaka, and Nobuo Ishiyama. Data analysis was performed by Yohei Arata. The first draft of the manuscript was written by Yohei Arata, and all authors commented on previous versions of the manuscript. All authors read and approved the final manuscript.

Figure captions

Figure 1. The study basin (Sorachi River Basin). (a) Location of the basin. (b) Elevation derived from. the 10 m resolution Digital Elevation Model provided by the Geospatial Information Authority of Japan. (c) Geological map derived from the 1:200,000 Seamless Geological Map of Japan (GeomapNAVI) provided by the Geological Survey of Japan, National Institute of Advanced Industrial Science and Technology. (d) Land use derived from the 10 m resolution High-Resolution Land Use and Land Cover Map (2018–2020, v21.11) provided by the Japan Aerospace Exploration Agency.

Figure 2. Schematic illustration of the analysis of climatic variables and hydrograph separation.

Figure 3. Model-averaged estimates from linear mixed models for quick discharge (a) and delayed discharge (b). Red shaded variables indicate statistical significance.

Figure 4. Three-dimensional plot showing the interaction between volcanic proportion and snowfall water equivalent for delayed discharge.

Figure 5. Spatial distribution of volcanic proportion and relief height for watersheds within the Sorachi River Basin. Watersheds were delineated using the Watershed tool in ArcGIS Pro version 3.1.0, with a minimum drainage area of 1 km^2.

Table captions

Table 1. Characteristics of monitoring watersheds.

Table 2. Model averaging for predicting quick discharge and delayed discharge.

Supplement captions

Figure S1. Workflow for calculating time-series discharge data.

Figure S2. Correlation matrix heatmap of covariates.

Figure S3. Mean hydrographs for all observed watersheds for each year. Mean precipitation and mean snow depth were derived from the Agro-Meteorological Grid Square Data provided by the National Agriculture and Food Research Organization.

Figure S4. Boxplots of snowfall water equivalent (SFWE), spring precipitation (Spring P), quick discharge (Q_q), and delayed discharge (Q_d) for each watershed.

Figure S5. Relationships between predicted and observed quick discharge (a) and delayed discharge (b).

Figure S6. Scatterplots of relationships identified as significant in the linear mixed model. The red shaded areas represent the 95% confidence intervals of the predicted values.

Figure S7. Mean hydrographs for watersheds with >90% and <10% volcanic proportion.

Table S1. Parameters for Manning's equation and roughness coefficient.

Table S2. Runoff characteristics for each watershed. Each variable represents the mean value. Annual values were calculated using only years in which hydrographs were available for more than 90% of the days.

Table S3. Model selection.

Table S4. Best model.

Text S1. Data collection of streamflow time-series data.

Text S2 Calculation of annual precipitation for each watershed.

Figure 1

Click here to access/download;colour figure;Figure 1.tiff

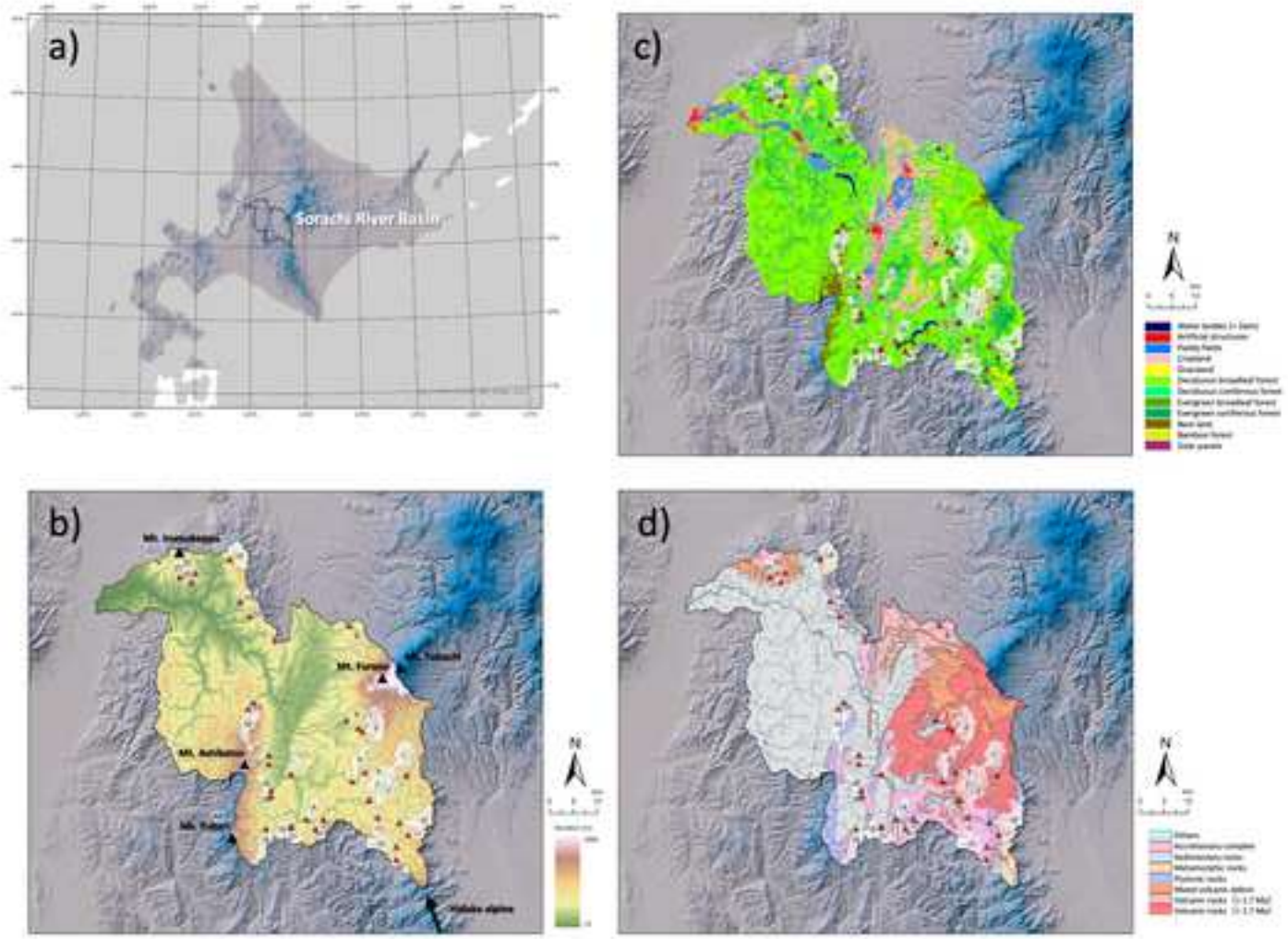


Figure 1

Figure 2

Click here to access/download;colour figure;Figure 2.tiff

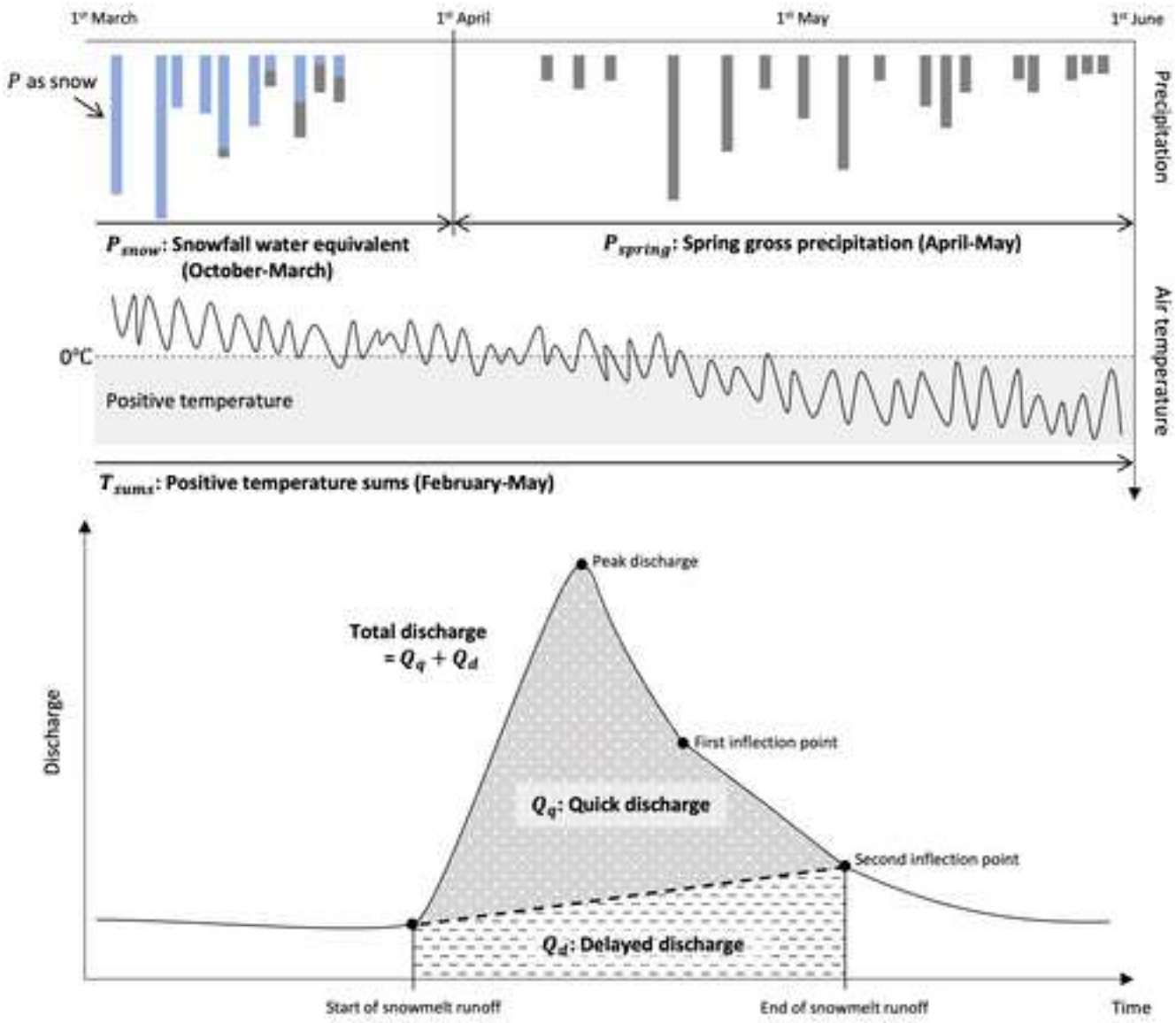


Figure 2

Figure 3

Click here to access/download;colour figure;Figure 3.tiff

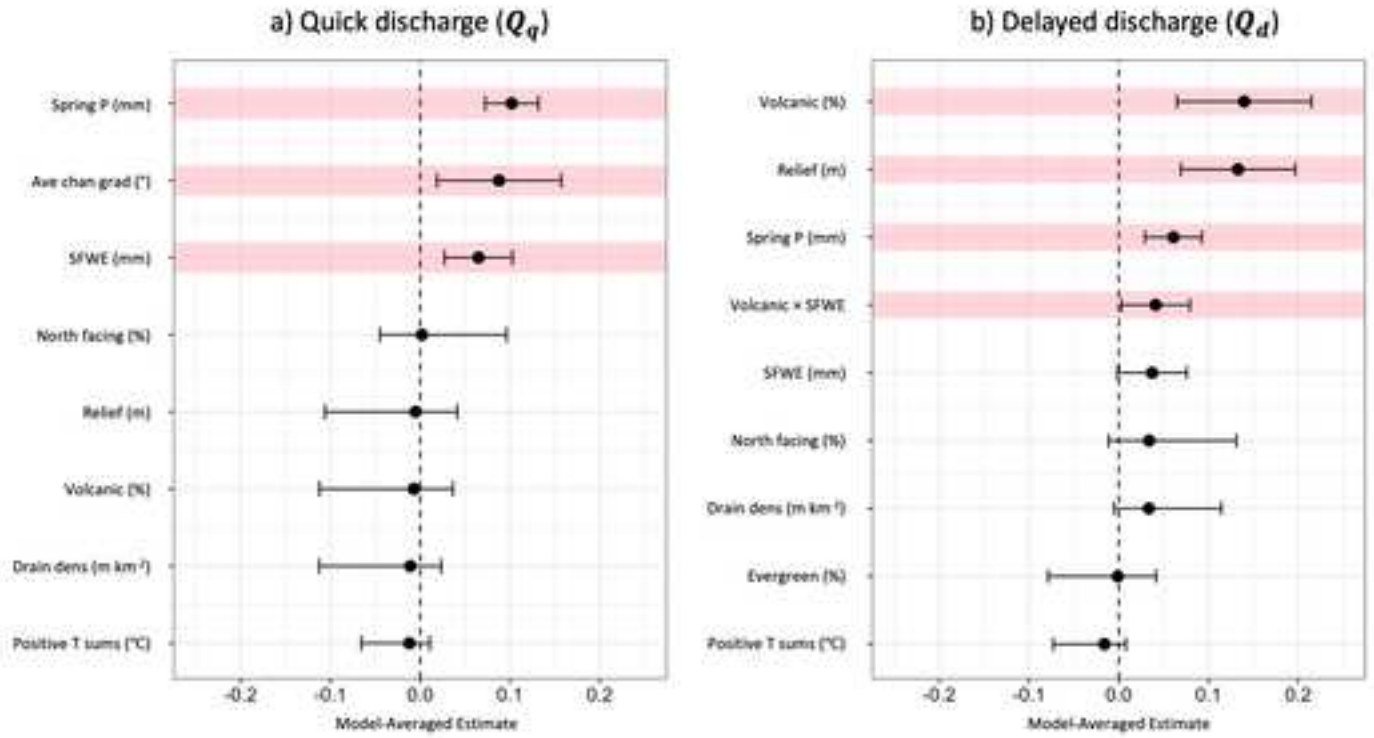


Figure 3

Figure 4

Click here to access/download;colour figure;Figure 4.tiff

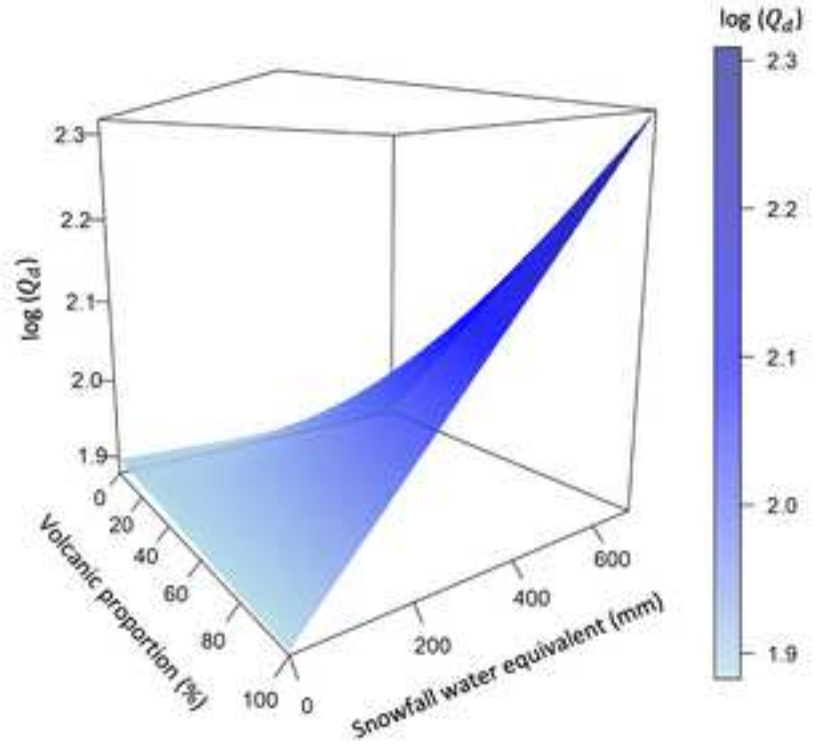


Figure 4

Figure 5

Click here to access/download;colour figure;Figure 5.tiff

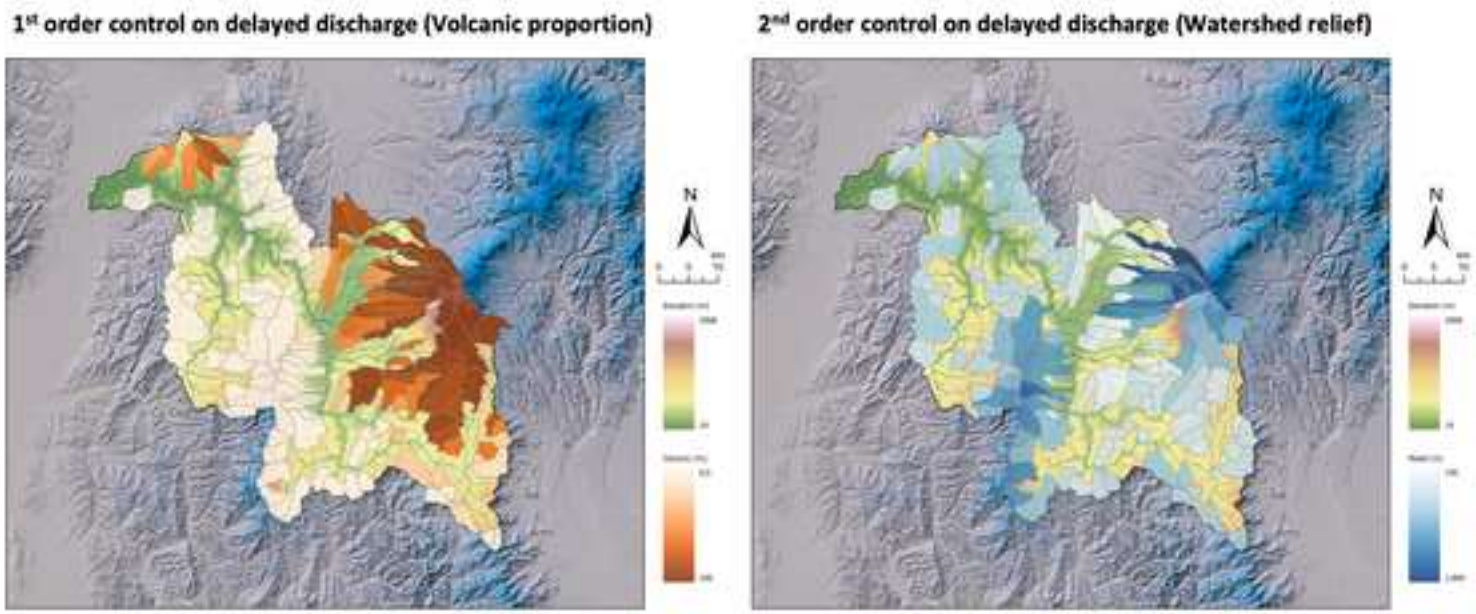


Figure 5

Table Click here to access/download;table;Table.xlsx

Table 1. Characteristics of monitoring watersheds.

Watershed	Area (km^2)	Volcanic rock (%)	Mean Elevation (m)	Relief (m)
ws1	21.9	98.9	732.9	420.1
ws2	19.3	88.0	574.7	497.9
ws3	16.4	95.7	559.0	414.1
ws4	15.7	63.3	530.6	513.9
ws5	3.3	99.3	616.0	729.5
ws6	3.1	100.0	485.9	291.6
ws7	8.3	100.0	869.9	1007.1
ws8	19.3	100.0	823.6	989.7
ws9	6.3	99.1	626.3	473.3
ws10	17.0	0.0	748.5	769.5
ws11	7.0	9.1	689.3	532.9
ws12	20.4	13.7	621.8	570.3
ws13	7.3	24.9	654.6	781.9
ws14	9.9	0.0	489.9	450.5
ws15	8.2	0.0	515.8	600.8
ws16	16.1	0.0	671.2	809.8
ws17	10.0	32.8	468.5	358.6
ws18	18.3	0.0	613.0	650.8
ws19	6.4	0.0	521.7	633.9
ws20	4.4	0.0	554.6	476.8
ws21	9.4	0.0	481.8	448.4
ws22	6.7	34.7	699.3	695.6
ws23	3.8	0.0	646.5	660.1
ws24	6.2	0.0	659.8	623.3
ws25	5.0	98.5	469.2	549.6
ws26	7.7	90.4	384.4	678.0
ws27	4.0	97.8	502.5	597.2
ws28	3.2	0.0	622.7	740.9
ws29	4.9	0.0	531.6	473.0
ws30	7.5	0.0	535.9	789.9
ws31	2.1	0.0	761.1	1023.4
ws32	19.3	0.0	809.1	1016.1
ws33	7.2	0.0	750.5	1020.7

Mean channel gradient (°)	Drainage density (m/km^2)	North facing (%)	Forest coverage (%)
8.9	2.08	33.4	92.8
6.6	1.88	37.1	64.8
8.3	2.06	26.9	78.5
7.2	1.78	24.3	99.3
8.5	2.77	8.5	98.5
9.5	2.06	51.4	87.4
15.6	1.86	18.7	93.2
9.1	1.50	20.1	92.1
12.2	1.79	40.6	97.2
10.6	1.76	37.1	90.9
8.6	2.14	48.4	89.0
7.0	1.82	44.8	92.8
12.0	1.76	68.0	97.4
10.6	1.88	31.0	98.6
10.3	1.89	44.8	99.3
13.0	1.90	42.0	99.3
11.7	1.67	34.9	98.8
16.0	1.79	34.5	98.1
14.6	1.86	25.8	99.7
14.1	1.54	31.8	98.0
8.7	1.80	44.7	98.8
6.1	2.19	50.4	90.5
19.7	1.75	59.1	99.9
15.6	1.82	48.5	99.1
10.4	2.12	10.7	96.1
9.5	1.92	21.1	91.6
10.4	1.39	26.7	94.7
21.8	1.46	55.5	96.8
16.0	1.69	41.6	96.8
13.4	1.97	42.1	93.8
19.5	2.57	41.0	83.7
19.6	1.77	50.5	82.9
10.4	1.99	42.7	71.9

Evergreen coverage (%)
23.1
16.5
27.3
6.8
11.6
2.4
23.6
18.5
17.9
17.2
16.9
13.7
26.5
23.2
6.2
9.3
11.4
1.1
6.8
9.4
10.4
25.4
12.1
1.8
38.9
45.7
15.6
11.5
5.7
12.1
18.1
17.2
1.7

Table 2. Model averaging for predicting quick discharge and delayed discharge.

Response	Covariate	Standardized coefficient	Std. Error
$Log_{10}(Qq)$	Intercept	2.1746	0.0328
	Snowfall water equivalent (mm)	0.0651	0.0192
	Spring precipitation (mm)	0.1021	0.0151
	Positive temperature sums (˚C)	-0.0119	0.0186
	Volcanic rock proportion (%)	-0.0068	0.0216
	Watershed relief (m)	-0.0052	0.0192
	Average channel gradient (°)	0.0880	0.0351
	Drainage density (m/km^2)	-0.0110	0.0257
	North facing proportion (%)	0.0020	0.0122
$Log_{10}(Qd)$	Intercept	2.0068	0.0288
	Snowfall water equivalent (mm)	0.0372	0.0195
	Spring precipitation (mm)	0.0610	0.0161
	Positive temperature sums (˚C)	-0.0160	0.0217
	Volcanic rock proportion (%)	0.1399	0.0380
	Watershed relief (m)	0.1330	0.0323
	Drainage density (m/km^2)	0.0335	0.0356
	North facing proportion (%)	0.0338	0.0402
	Evergreen proportion (%)	-0.0011	0.0087
	Volcanic × Snowfall water equivalent	0.0411	0.0193

[a] Not significant

Adjusted SE	95%CI	z	p	Sum of weights
0.0331	2.110 to 2.239	65.694	< 0.001	-
0.0193	0.027 to 0.103	3.365	< 0.001	0.99
0.0152	0.072 to 0.132	6.734	< 0.001	1.00
0.0187	-0.066 to 0.011	0.637	n.s.[a]	0.50
0.0217	-0.112 to 0.036	0.315	n.s.	0.56
0.0193	-0.106 to 0.041	0.272	n.s.	0.30
0.0354	0.019 to 0.157	2.488	< 0.05	0.78
0.0258	-0.113 to 0.024	0.426	n.s.	0.42
0.0122	-0.045 to 0.096	0.165	n.s.	0.27
0.0291	1.950 to 2.064	69.081	< 0.001	-
0.0197	-0.0013 to 0.076	1.892	n.s.	0.92
0.0162	0.029 to 0.093	3.765	< 0.001	1.00
0.0218	-0.073 to 0.0079	0.736	n.s.	0.50
0.0382	0.065 to 0.215	3.659	< 0.001	1.00
0.0325	0.069 to 0.197	4.091	< 0.001	0.99
0.0357	-0.0052 to 0.114	0.937	n.s.	0.54
0.0403	-0.011 to 0.131	0.838	n.s.	0.50
0.0088	-0.079 to 0.042	0.128	n.s.	0.25
0.0195	0.0029 to 0.079	2.110	< 0.05	0.66

Figure S1

Click here to access/download;attachment to manuscript;Figure S1.tiff

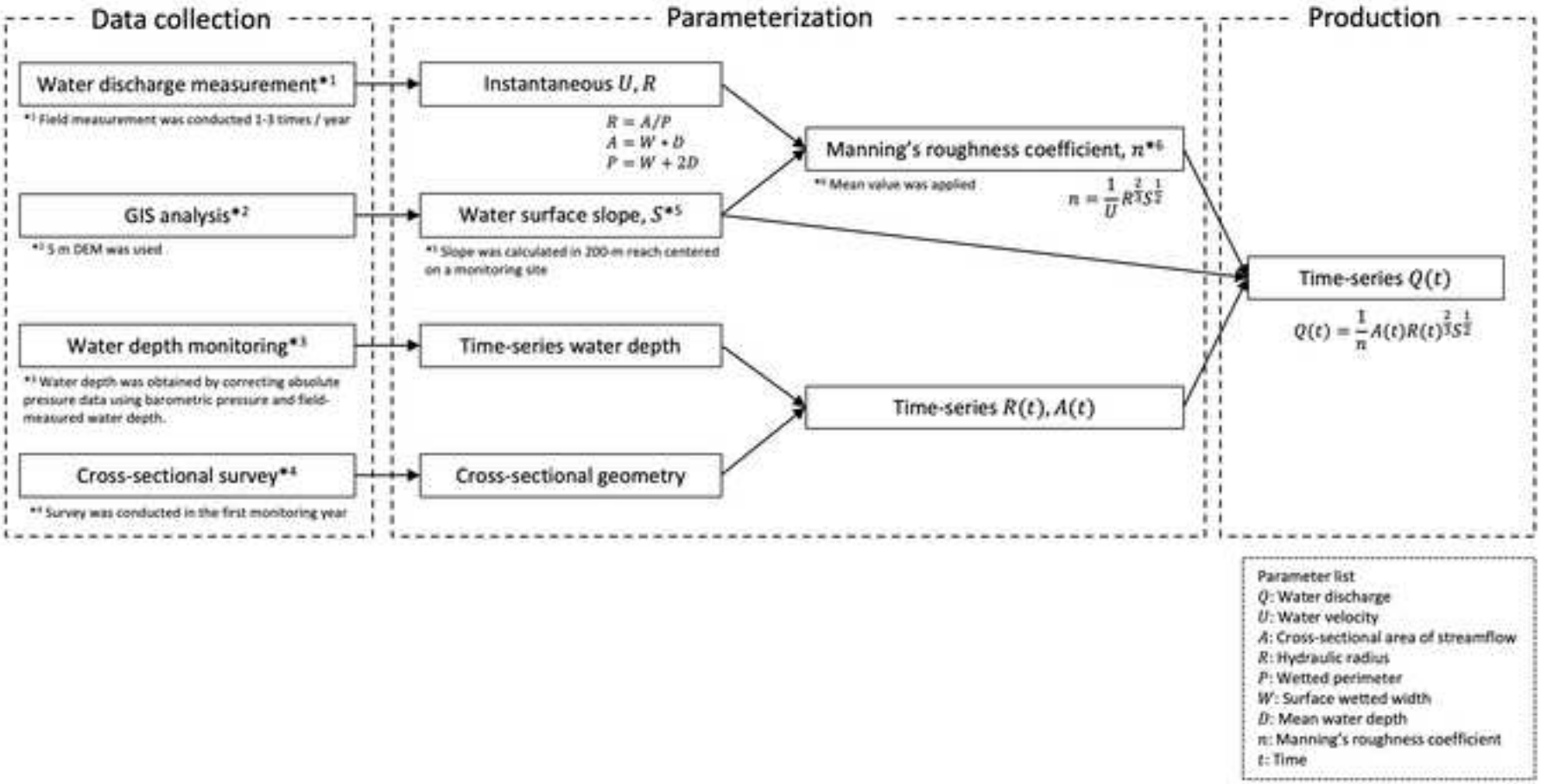


Figure S1

Figure S2

Click here to access/download;attachment to manuscript;Figure S2.tiff

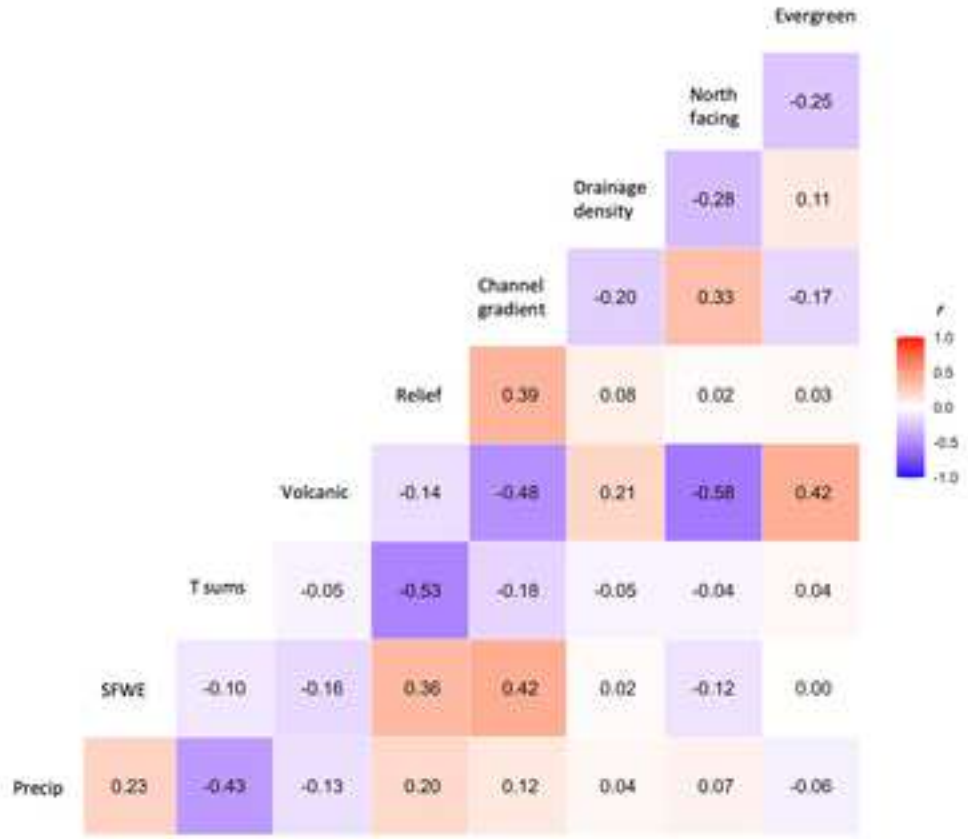


Figure S2

Figure S3

Click here to access/download;attachment to manuscript;Figure S3.tiff

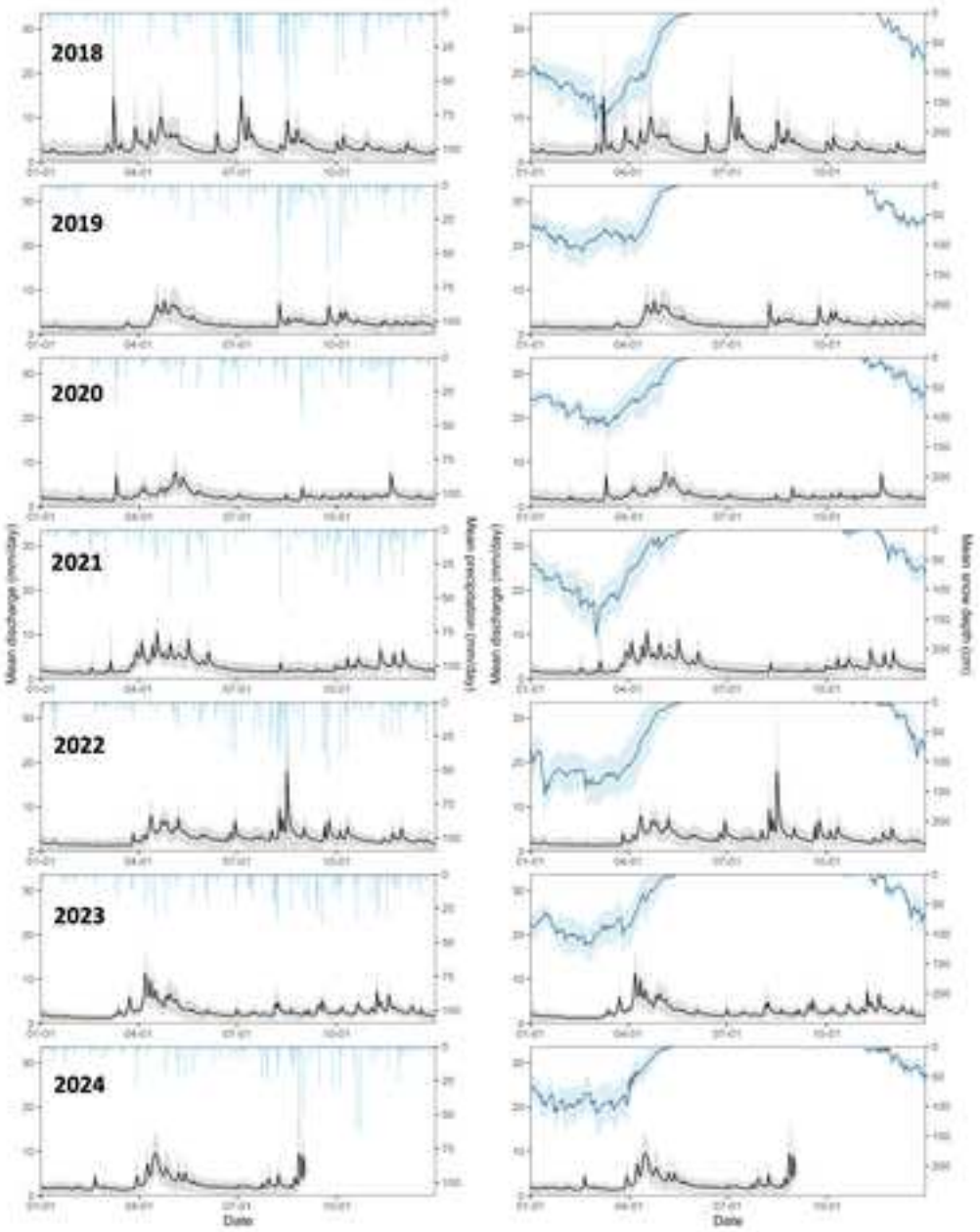


Figure S3

Figure S4

Click here to access/download;attachment to manuscript;Figure S4.tiff

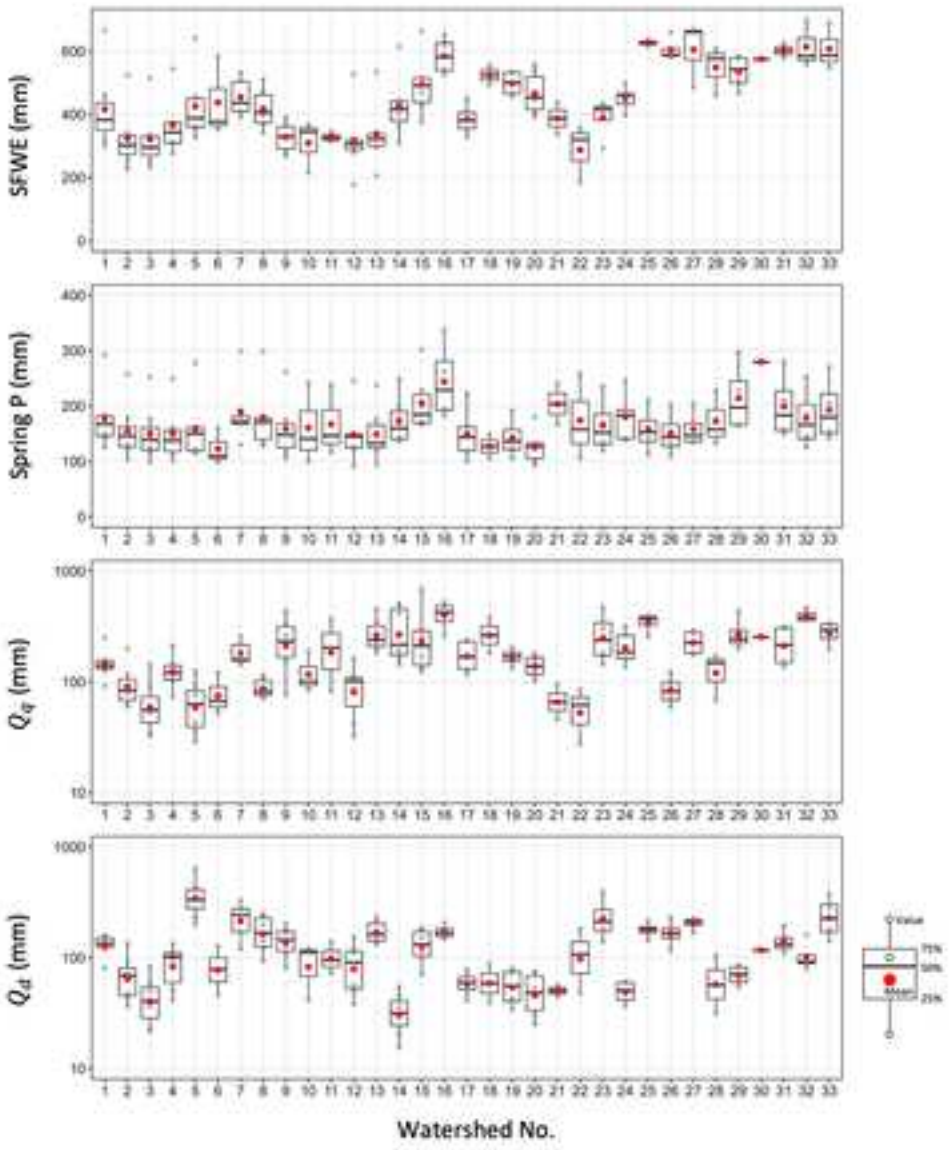


Figure S4

Figure S5

Click here to access/download;attachment to manuscript;Figure S5.tiff

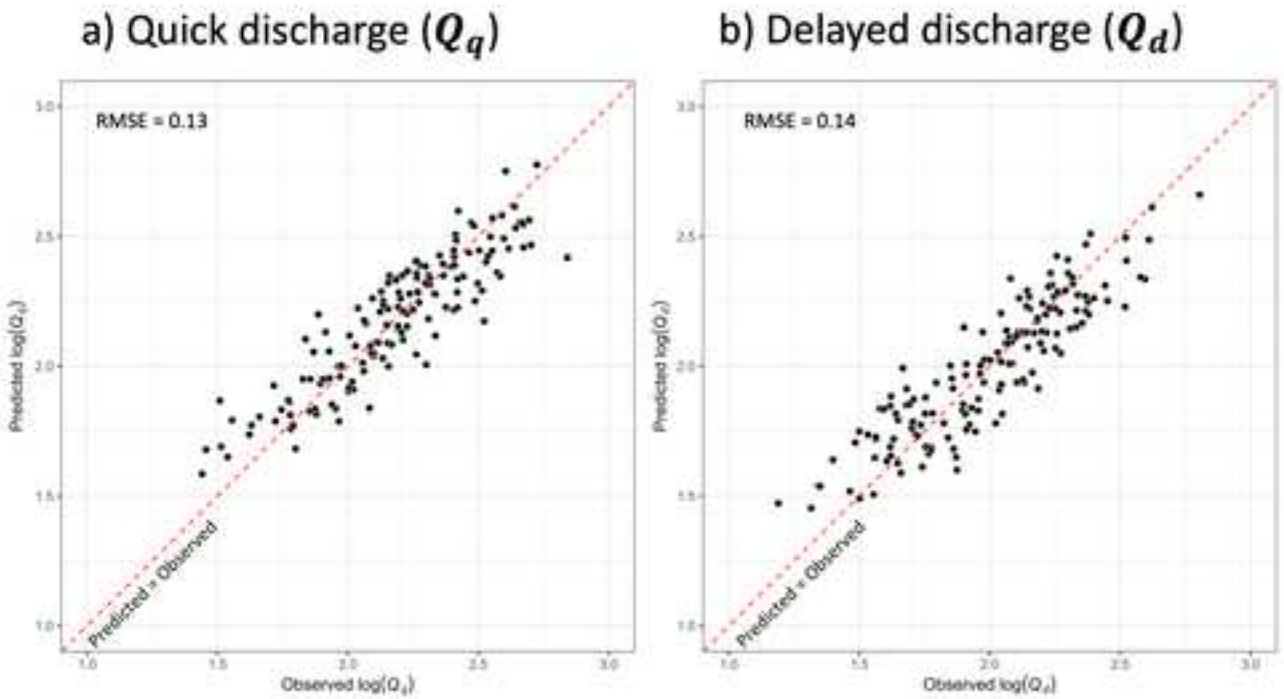


Figure S5

Figure S6

Click here to access/download;attachment to manuscript;Figure S6.tiff

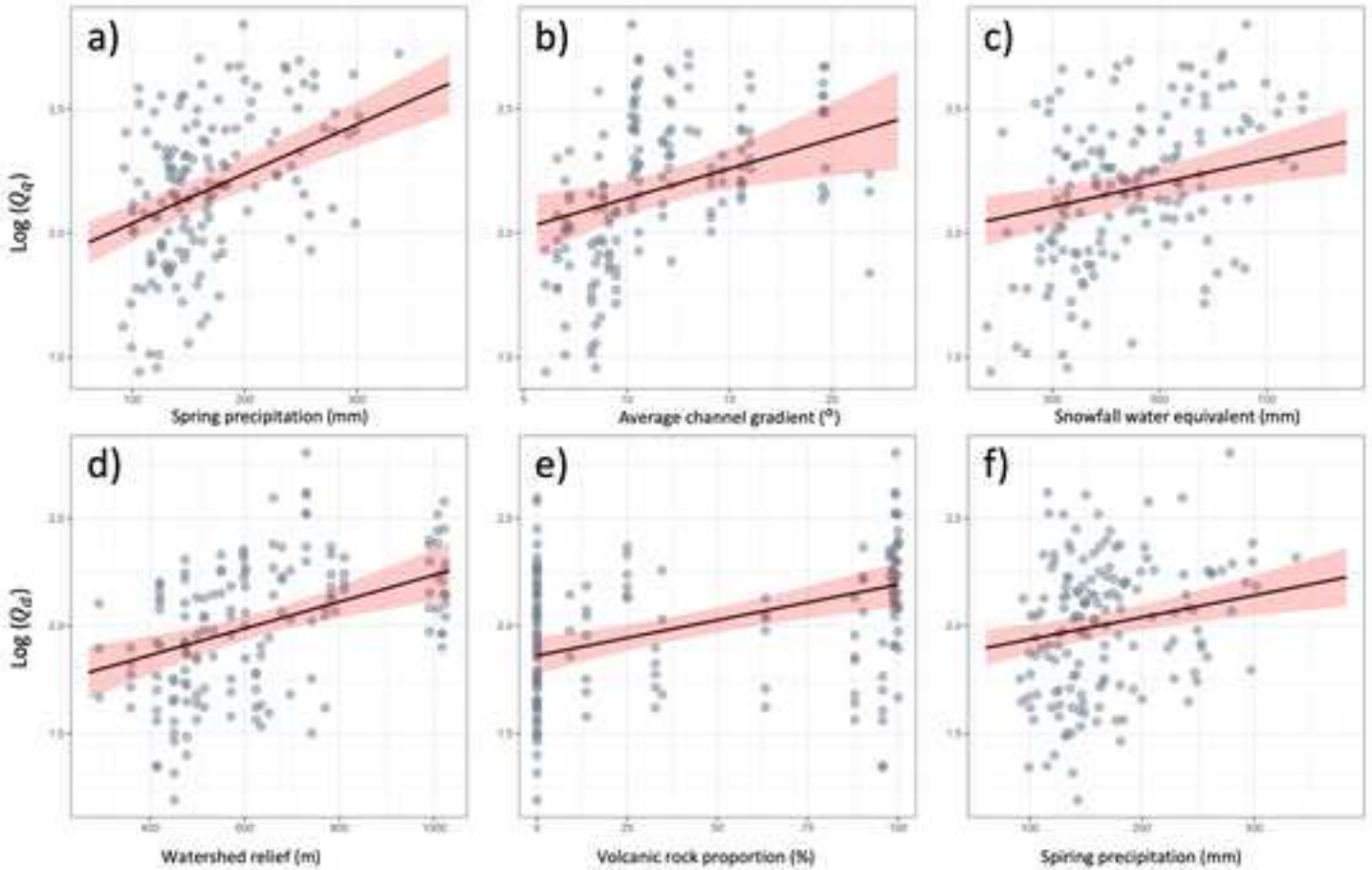


Figure S6

Figure S7

Click here to access/download;attachment to manuscript;Figure S7.tiff

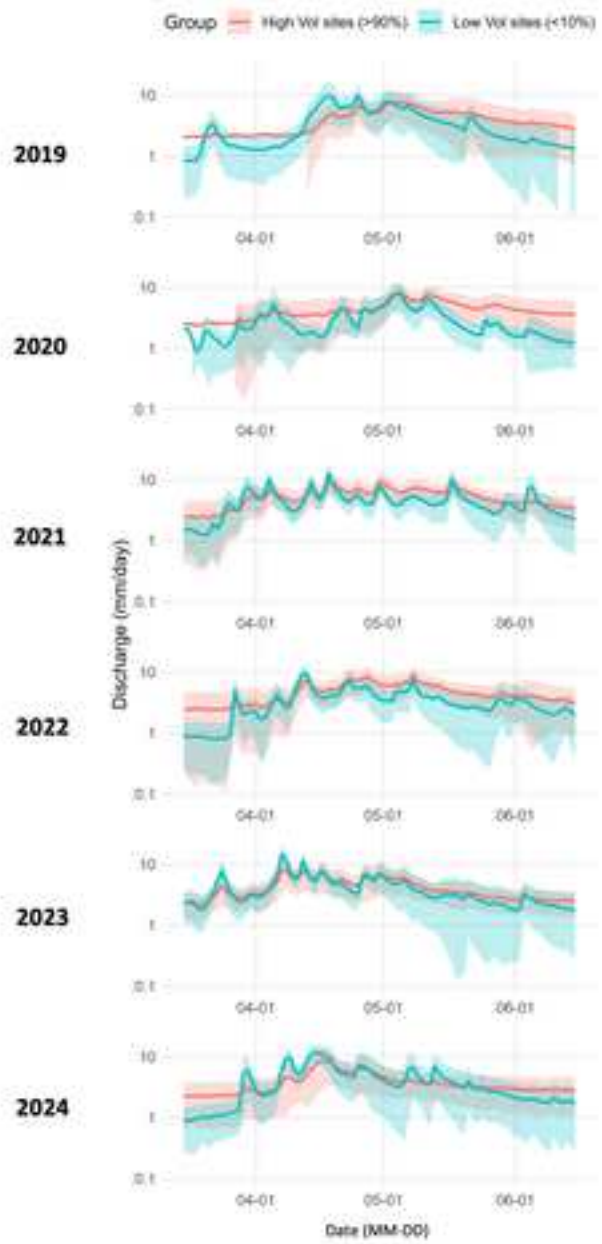


Figure S7

Click here to access/download;attachment to manuscript;Table_SI.xlsx

Table S1. Paramteers for Manning's equation and roughness coefficient.

	Date	Time	*W (m)*	*D (m)*	A (m^2)	*P (m)*	*R (m)*	*S (m/m)*	*Q* (m^3/*s*)	*V (m/s)*	*n*
ws1	6/22/2020	15:30	3.8	0.24	0.88	4.22	0.21	0.0225	0.322	0.36	0.145
	8/13/2020	9:40	3.6	0.21	0.77	4.03	0.19	0.0225	0.268	0.35	0.144
	10/26/2020	12:05	5.7	0.17	0.95	5.99	0.16	0.0225	0.562	0.59	0.074
	5/26/2021	12:00	6.6	0.26	1.74	7.13	0.24	0.0225	1.592	0.92	0.064
	10/20/2021	11:30	5.2	0.26	1.33	5.71	0.23	0.0225	0.600	0.45	0.126
	9/29/2022	11:55	5.5	0.32	1.77	6.14	0.29	0.0225	1.112	0.63	0.104
	7/25/2023	11:28	4.0	0.26	1.04	4.52	0.23	0.0225	0.217	0.21	0.270
		Mean	4.9	0.25	1.21	5.39	0.22	0.0225	0.668	0.50	**0.132**
ws2	6/22/2020	14:34	7.0	0.18	1.23	7.35	0.17	0.0155	0.277	0.23	0.167
	8/13/2020	8:50	6.8	0.17	1.16	7.14	0.16	0.0155	0.219	0.19	0.195
	10/26/2020	11:35	6.3	0.22	1.37	6.74	0.20	0.0155	0.397	0.29	0.149
	5/26/2021	14:00	7.0	0.23	1.61	7.46	0.22	0.0155	0.927	0.57	0.078
	10/20/2021	10:30	6.5	0.24	1.55	6.98	0.22	0.0155	0.504	0.33	0.140
	9/29/2022	11:20	7.0	0.20	1.42	7.41	0.19	0.0155	0.925	0.65	0.064
	7/25/2023	10:40	4.5	0.21	0.94	4.92	0.19	0.0155	0.194	0.21	0.200
		Mean	6.4	0.21	1.33	6.86	0.19	0.0155	0.492	0.35	**0.142**
ws3	6/22/2020	14:14	5.0	0.20	1.00	5.40	0.18	0.0631	0.195	0.20	0.416
	8/13/2020	8:50	2.7	0.23	0.61	3.15	0.19	0.0631	0.171	0.28	0.298
	10/26/2020	11:20	3.0	0.31	0.93	3.62	0.26	0.0631	0.127	0.14	0.742
	10/20/2021	10:10	3.7	0.34	1.25	4.37	0.28	0.0631	0.276	0.22	0.491
	9/29/2022	10:57	5.5	0.29	1.57	6.07	0.26	0.0631	0.765	0.49	0.210
	7/25/2023	10:19	3.0	0.18	0.54	3.36	0.16	0.0631	0.138	0.26	0.290
		Mean	3.8	0.26	0.98	4.33	0.22	0.0631	0.279	0.26	**0.408**
ws4	6/22/2020	13:41	4.5	0.10	0.45	4.70	0.10	0.0070	0.187	0.41	0.043
	8/12/2020	11:56	3.0	0.11	0.34	3.18	0.11	0.0070	0.124	0.37	0.051
	10/26/2020	10:27	2.9	0.13	0.39	3.17	0.12	0.0070	0.116	0.30	0.069
	8/4/2021	9:46	3.2	0.11	0.36	3.43	0.11	0.0070	0.106	0.29	0.063
	10/20/2021	12:40	4.5	0.16	0.72	4.82	0.15	0.0070	0.347	0.48	0.049
	9/14/2022	10:30	3.9	0.15	0.59	4.20	0.14	0.0070	0.257	0.43	0.052
	7/25/2023	9:45	4.0	0.11	0.43	4.21	0.10	0.0070	0.102	0.24	0.076
		Mean	3.7	0.13	0.47	3.96	0.12	0.0070	0.177	0.36	**0.058**
ws5	6/22/2020	10:40	2.5	0.10	0.25	2.70	0.09	0.0588	0.217	0.88	0.056
	8/12/2020	9:55	1.9	0.15	0.29	2.21	0.13	0.0588	0.311	1.07	0.059
	10/27/2020	15:55	2.1	0.16	0.33	2.42	0.14	0.0588	0.197	0.60	0.108
	6/1/2021	10:15	2.7	0.15	0.41	3.01	0.14	0.0588	0.298	0.72	0.090
	10/20/2021	15:10	1.7	0.13	0.22	1.91	0.11	0.0588	0.180	0.83	0.069
	9/14/2022	13:30	2.3	0.15	0.35	2.60	0.13	0.0588	0.225	0.65	0.098
	10/15/2022	13:25	2.6	0.09	0.24	2.74	0.09	0.0588	0.253	1.06	0.045
	8/28/2023	12:20	1.8	0.19	0.35	2.19	0.16	0.0588	0.269	0.78	0.092
		Mean	2.2	0.14	0.30	2.47	0.12	0.0588	0.244	0.82	**0.077**
ws6	6/25/2020	16:10	1.3	0.13	0.16	1.55	0.10	0.0546	0.075	0.46	0.113
	8/11/2020	12:40	1.2	0.15	0.18	1.50	0.12	0.0546	0.086	0.47	0.121
	10/28/2020	13:55	1.5	0.10	0.14	1.69	0.08	0.0546	0.065	0.46	0.098
		Mean	1.3	0.12	0.16	1.58	0.10	0.0546	0.075	0.46	**0.111**
ws7	6/22/2020	11:30	2.4	0.18	0.44	2.77	0.16	0.0740	0.253	0.57	0.139
	8/12/2020	10:13	2.3	0.15	0.34	2.59	0.13	0.0740	0.186	0.55	0.126
	10/27/2020	15:20	2.1	0.14	0.30	2.39	0.13	0.0740	0.169	0.57	0.121
	6/1/2021	11:00	3.3	0.20	0.65	3.70	0.18	0.0740	0.549	0.84	0.102
	10/20/2021	14:45	2.1	0.18	0.38	2.47	0.16	0.0740	0.245	0.64	0.123
	9/14/2022	12:50	3.3	0.18	0.59	3.66	0.16	0.0740	0.297	0.51	0.158
	8/28/2023	11:39	3.0	0.22	0.67	3.45	0.19	0.0740	0.289	0.43	0.211
		Mean	2.6	0.18	0.48	3.00	0.16	0.0740	0.284	0.59	**0.140**
ws8	6/22/2020	11:56	5.0	0.17	0.85	5.34	0.16	0.0361	0.531	0.63	0.089
	8/12/2020	10:30	5.2	0.14	0.75	5.49	0.14	0.0361	0.550	0.73	0.069
	10/27/2020	14:50	5.3	0.17	0.89	5.64	0.16	0.0361	0.470	0.53	0.105
	6/1/2021	12:55	4.2	0.35	1.47	4.90	0.30	0.0361	1.355	0.92	0.092
	10/20/2021	14:00	5.0	0.23	1.15	5.46	0.21	0.0361	0.892	0.78	0.087
	9/14/2022	12:00	4.9	0.16	0.81	5.23	0.15	0.0361	0.545	0.68	0.081
	8/28/2023	11:10	6.0	0.16	0.98	6.33	0.15	0.0361	0.520	0.53	0.103

		Mean	5.1	0.20	0.98	5.48	0.18	0.0361	0.695	0.69	**0.089**
ws9	6/22/2020	13:15	3.1	0.14	0.43	3.38	0.13	0.0562	0.185	0.43	0.138
	8/12/2020	11:20	2.5	0.14	0.34	2.77	0.12	0.0562	0.133	0.39	0.148
	10/28/2020	10:52	2.7	0.18	0.49	3.06	0.16	0.0562	0.136	0.28	0.253
	6/1/2021	14:05	3.3	0.18	0.60	3.67	0.16	0.0562	0.445	0.74	0.096
	10/20/2021	13:10	3.8	0.17	0.65	4.14	0.16	0.0562	0.121	0.19	0.365
	9/14/2022	11:05	3.5	0.16	0.56	3.82	0.15	0.0562	0.290	0.51	0.129
	10/15/2022	12:15	4.3	0.18	0.78	4.66	0.17	0.0562	0.439	0.56	0.129
	8/28/2023	10:12	3.5	0.13	0.46	3.76	0.12	0.0562	0.201	0.44	0.134
		Mean	3.3	0.16	0.54	3.66	0.15	0.0562	0.244	0.44	**0.174**
ws10	6/23/2020	9:43	4.5	0.16	0.69	4.76	0.14	0.0410	0.338	0.49	0.114
	8/13/2020	11:35	4.4	0.14	0.60	4.63	0.13	0.0410	0.296	0.49	0.105
	10/26/2020	14:32	5.3	0.16	0.85	5.62	0.15	0.0410	0.502	0.59	0.097
	10/21/2021	15:10	5.4	0.26	1.41	5.92	0.24	0.0410	1.445	1.03	0.076
	7/25/2023	13:46	5.7	0.18	1.04	6.06	0.17	0.0410	0.473	0.45	0.137
		Mean	5.0	0.18	0.92	5.40	0.17	0.0410	0.611	0.61	**0.106**
ws11	6/22/2020	17:25	4.0	0.11	0.42	4.21	0.10	0.0612	0.203	0.48	0.111
	8/13/2020	10:27	3.9	0.12	0.47	4.09	0.11	0.0612	0.228	0.49	0.119
	10/26/2020	14:08	4.0	0.14	0.57	4.29	0.13	0.0612	0.347	0.60	0.107
	10/21/2021	14:40	4.3	0.16	0.70	4.63	0.15	0.0612	0.543	0.77	0.091
	9/29/2022	14:45	4.8	0.12	0.57	5.04	0.11	0.0612	0.458	0.80	0.072
	7/25/2023	12:50	4.7	0.10	0.46	4.89	0.09	0.0612	0.166	0.37	0.139
		Mean	4.3	0.12	0.53	4.52	0.12	0.0612	0.324	0.59	**0.107**
ws12	6/22/2020	16:20	5.0	0.22	1.09	5.44	0.20	0.0429	0.393	0.36	0.197
	8/13/2020	10:27	5.2	0.26	1.32	5.66	0.23	0.0429	0.457	0.35	0.227
	10/26/2020	13:00	4.5	0.25	1.10	4.99	0.22	0.0429	0.807	0.73	0.103
	10/21/2021	14:00	8.5	0.26	2.23	9.02	0.25	0.0429	1.885	0.85	0.096
	9/29/2022	13:05	5.3	0.36	1.89	6.01	0.31	0.0429	1.021	0.54	0.177
	7/25/2023	12:24	6.0	0.19	1.14	6.38	0.18	0.0429	0.343	0.30	0.218
		Mean	5.7	0.25	1.46	6.25	0.23	0.0429	0.818	0.52	**0.170**
ws13	6/23/2020	10:00	2.0	0.16	0.33	2.33	0.14	0.0330	0.196	0.60	0.082
	8/13/2020	12:35	2.0	0.06	0.13	2.13	0.06	0.0330	0.069	0.55	0.050
	10/26/2020	13:40	2.3	0.12	0.28	2.54	0.11	0.0330	0.171	0.62	0.067
	5/26/2021	15:00	4.5	0.15	0.66	4.79	0.14	0.0330	0.410	0.62	0.077
	10/21/2021	13:25	4.9	0.17	0.85	5.25	0.16	0.0330	0.631	0.75	0.072
	9/29/2022	13:53	3.3	0.14	0.47	3.59	0.13	0.0330	0.429	0.91	0.051
	7/25/2023	14:20	3.0	0.09	0.28	3.19	0.09	0.0330	0.107	0.38	0.093
		Mean	3.1	0.13	0.43	3.40	0.12	0.0330	0.288	0.63	**0.070**
ws14	6/25/2020	11:53	1.6	0.11	0.17	1.82	0.10	0.0330	0.059	0.34	0.111
	8/13/2020	13:00	1.6	0.07	0.12	1.75	0.07	0.0330	0.042	0.35	0.085
	10/27/2020	9:51	1.9	0.14	0.26	2.17	0.12	0.0330	0.063	0.25	0.177
	6/1/2021	15:20	1.9	0.22	0.43	2.35	0.18	0.0330	0.334	0.79	0.074
	10/21/2021	10:40	5.5	0.39	2.12	6.27	0.34	0.0330	1.832	0.87	0.102
	9/30/2022	10:45	3.7	0.12	0.45	3.94	0.11	0.0330	0.181	0.40	0.105
	7/26/2023	9:09	2.3	0.11	0.25	2.51	0.10	0.0330	0.073	0.30	0.130
		Mean	2.6	0.16	0.54	2.97	0.14	0.0330	0.369	0.47	**0.112**
ws15	10/27/2020	8:42	2.6	0.21	0.54	3.01	0.18	0.0391	0.121	0.23	0.278
	10/21/2021	9:40	5.0	0.34	1.68	5.67	0.30	0.0391	1.271	0.76	0.116
	9/30/2022	8:47	3.7	0.14	0.50	3.97	0.13	0.0391	0.238	0.47	0.105
	7/26/2023	7:20	3.2	0.13	0.42	3.46	0.12	0.0391	0.083	0.20	0.242
		Mean	3.6	0.20	0.78	4.03	0.18	0.0391	0.428	0.41	**0.185**
ws16	6/23/2020	14:00	5.5	0.13	0.72	5.76	0.13	0.0240	0.199	0.27	0.142
	8/12/2020	14:48	8.0	0.18	1.43	8.36	0.17	0.0240	0.716	0.50	0.096
	10/27/2020	12:20	6.2	0.16	1.00	6.47	0.15	0.0240	0.347	0.35	0.128
	10/22/2021	9:30	9.0	0.26	2.38	9.53	0.25	0.0240	1.981	0.83	0.074
	9/30/2022	9:45	5.0	0.18	0.88	5.35	0.16	0.0240	0.692	0.79	0.059
	7/26/2023	8:20	5.2	0.16	0.81	5.51	0.15	0.0240	0.465	0.57	0.076
		Mean	6.5	0.18	1.20	6.83	0.17	0.0240	0.733	0.55	**0.096**
ws17	6/23/2020	15:20	2.2	0.10	0.23	2.41	0.09	0.0635	0.058	0.26	0.205
	8/11/2020	14:40	2.0	0.10	0.20	2.20	0.09	0.0635	0.044	0.22	0.230
	10/26/2020	9:50	2.5	0.11	0.27	2.72	0.10	0.0635	0.054	0.20	0.269
	6/1/2021	16:15	2.7	0.16	0.43	3.02	0.14	0.0635	0.173	0.40	0.174

	10/21/2021	8:30	3.5	0.21	0.73	3.92	0.19	0.0635	0.510	0.70	0.118
	8/28/2023	9:29	2.0	0.13	0.26	2.26	0.12	0.0635	0.075	0.29	0.208
		Mean	2.5	0.14	0.35	2.75	0.12	0.0635	0.152	0.34	**0.201**
ws18	6/26/2020	12:50	4.2	0.30	1.26	4.80	0.26	0.0675	0.180	0.14	0.744
	8/11/2020	10:00	4.0	0.39	1.55	4.78	0.32	0.0675	0.276	0.18	0.691
	10/22/2020	14:23	4.0	0.31	1.24	4.62	0.27	0.0675	0.149	0.12	0.905
	5/27/2021	14:00	4.8	0.37	1.75	5.53	0.32	0.0675	0.501	0.29	0.423
		Mean	4.3	0.34	1.45	4.93	0.29	0.0675	0.277	0.18	**0.691**
ws19	6/26/2020	11:00	2.3	0.11	0.26	2.53	0.10	0.0709	0.047	0.18	0.331
	8/11/2020	11:00	2.3	0.10	0.23	2.50	0.09	0.0709	0.055	0.24	0.232
	10/28/2020	15:27	2.3	0.12	0.28	2.55	0.11	0.0709	0.073	0.26	0.241
	11/2/2021	10:15	2.8	0.11	0.31	2.98	0.10	0.0709	0.074	0.24	0.247
	9/13/2022	13:19	1.8	0.11	0.20	2.02	0.10	0.0709	0.040	0.20	0.277
	7/17/2023	13:50	2.7	0.12	0.31	2.88	0.11	0.0709	0.087	0.28	0.215
		Mean	2.4	0.11	0.27	2.58	0.10	0.0709	0.063	0.23	**0.257**
ws20	6/26/2020	11:33	2.0	0.11	0.22	2.22	0.10	0.0590	0.030	0.14	0.380
	8/11/2020	11:35	2.1	0.12	0.25	2.34	0.11	0.0590	0.045	0.18	0.305
	11/2/2021	9:40	2.1	0.13	0.27	2.36	0.11	0.0590	0.073	0.27	0.212
	9/13/2022	14:07	2.1	0.12	0.24	2.29	0.11	0.0590	0.027	0.11	0.486
	10/6/2022	13:53	2.6	0.14	0.37	2.89	0.13	0.0590	0.130	0.35	0.180
	7/17/2023	12:55	2.5	0.12	0.30	2.74	0.11	0.0590	0.049	0.16	0.334
		Mean	2.2	0.12	0.28	2.47	0.11	0.0590	0.059	0.20	**0.316**
ws21	6/25/2020	9:20	2.3	0.10	0.23	2.50	0.09	0.0110	0.055	0.24	0.088
	8/12/2020	0:00	2.7	0.11	0.28	2.86	0.10	0.0110	0.090	0.32	0.070
	10/27/2020	9:21	2.5	0.13	0.33	2.76	0.12	0.0110	0.127	0.38	0.066
	10/21/2021	9:50	7.5	0.26	1.98	8.03	0.25	0.0110	1.611	0.81	0.051
		Mean	3.7	0.15	0.71	4.04	0.14	0.0110	0.471	0.44	**0.069**
ws22	6/23/2020	9:00	4.3	0.10	0.43	4.50	0.10	0.0311	0.154	0.36	0.103
	8/13/2020	10:27	3.4	0.09	0.31	3.53	0.09	0.0311	0.116	0.38	0.091
	10/26/2020	15:06	3.5	0.11	0.39	3.72	0.10	0.0311	0.155	0.40	0.097
	10/21/2021	15:35	4.5	0.16	0.72	4.82	0.15	0.0311	0.433	0.60	0.082
		Mean	3.9	0.12	0.46	4.14	0.11	0.0311	0.214	0.44	**0.093**
ws23	6/23/2020	12:22	2.2	0.11	0.24	2.42	0.10	0.0830	0.072	0.30	0.206
	8/12/2020	16:30	2.2	0.10	0.21	2.39	0.09	0.0830	0.051	0.24	0.235
	10/27/2020	11:30	2.3	0.13	0.29	2.55	0.11	0.0830	0.070	0.24	0.281
	10/21/2021	11:30	2.7	0.22	0.60	3.14	0.19	0.0830	0.501	0.84	0.113
	9/30/2022	12:20	3.5	0.12	0.42	3.74	0.11	0.0830	0.193	0.47	0.143
	7/25/2023	15:54	2.3	0.1	0.19	2.47	0.08	0.0830	0.061	0.31	0.168
		Mean	2.5	0.13	0.32	2.79	0.11	0.0830	0.158	0.40	**0.191**
ws24	6/23/2020	11:45	1.9	0.16	0.30	2.22	0.14	0.1149	0.080	0.26	0.340
	8/12/2020	17:30	2.4	0.20	0.47	2.79	0.17	0.1149	0.120	0.26	0.404
	10/27/2020	10:40	2.5	0.19	0.49	2.89	0.17	0.1149	0.113	0.23	0.445
	10/21/2021	12:00	4.5	0.26	1.17	5.02	0.23	0.1149	0.913	0.78	0.166
	9/30/2022	13:25	2.6	0.19	0.49	2.94	0.17	0.1149	0.300	0.61	0.171
	7/25/2023	15:27	2.0	0.15	0.29	2.29	0.13	0.1149	0.105	0.36	0.235
		Mean	2.6	0.19	0.54	3.02	0.17	0.1149	0.272	0.42	**0.293**
ws25	11/1/2021	11:10	2.4	0.08	0.19	2.56	0.08	0.0699	0.097	0.50	0.094
	5/31/2022	9:24	2.6	0.16	0.41	2.91	0.14	0.0699	0.194	0.48	0.150
	9/13/2022	9:08	2.4	0.08	0.20	2.57	0.08	0.0699	0.119	0.59	0.083
	7/26/2023	13:06	2.1	0.10	0.21	2.26	0.09	0.0699	0.091	0.43	0.127
		Mean	2.4	0.11	0.25	2.58	0.10	0.0699	0.125	0.50	**0.114**
ws26	11/1/2021	12:00	3.9	0.25	0.96	4.39	0.22	0.025	0.134	0.14	0.412
	5/31/2022	10:40	5.0	0.13	0.66	5.27	0.13	0.025	0.243	0.37	0.109
	9/13/2022	10:25	3.0	0.20	0.60	3.40	0.18	0.025	0.151	0.25	0.196
	7/26/2023	11:40	3.8	0.12	0.47	4.05	0.12	0.025	0.128	0.27	0.139
		Mean	3.9	0.18	0.67	4.28	0.16	0.0250	0.164	0.26	**0.214**
ws27	6/26/2020	14:00	1.3	0.13	0.17	1.56	0.11	0.0851	0.112	0.65	0.102
	8/11/2020	9:30	1.2	0.19	0.22	1.54	0.15	0.0851	0.131	0.59	0.137
	10/22/2020	15:20	1.0	0.21	0.21	1.42	0.15	0.0851	0.106	0.51	0.161
	5/27/2021	13:20	2.1	0.20	0.41	2.49	0.17	0.0851	0.217	0.53	0.167
	11/1/2021	13:44	1.8	0.15	0.27	2.10	0.13	0.0851	0.121	0.45	0.168
	9/13/2022	11:47	1.8	0.12	0.22	2.05	0.11	0.0851	0.097	0.44	0.153

	10/6/2022	12:52	2.1	0.19	0.41	2.49	0.16	0.0851	0.199	0.49	0.179
	7/17/2023	14:50	1.8	0.19	0.34	2.17	0.15	0.0851	0.117	0.35	0.241
		Mean	1.6	0.17	0.28	1.98	0.14	0.0851	0.138	0.50	**0.163**
ws28	5/19/2020	9:35	2.8	0.10	0.29	2.96	0.10	0.0785	0.131	0.46	0.129
	6/25/2020	9:56	2.5	0.09	0.21	2.67	0.08	0.0785	0.067	0.32	0.164
	8/13/2020	14:50	1.9	0.07	0.14	2.05	0.07	0.0785	0.021	0.16	0.298
	10/28/2020	11:25	2.0	0.10	0.21	2.21	0.09	0.0785	0.023	0.11	0.521
	5/27/2021	9:30	1.8	0.15	0.28	2.11	0.13	0.0785	0.154	0.56	0.129
	8/4/2021	13:34	1.8	0.08	0.14	1.95	0.07	0.0785	0.018	0.13	0.381
	10/22/2021	14:40	2.4	0.11	0.26	2.62	0.10	0.0785	0.084	0.33	0.184
	9/14/2022	15:03	2.0	0.09	0.17	2.13	0.08	0.0785	0.041	0.24	0.215
	7/16/2023	9:50	2.2	0.11	0.24	2.42	0.10	0.0785	0.068	0.29	0.210
		Mean	2.1	0.10	0.21	2.34	0.09	0.0785	0.068	0.29	**0.248**
ws29	5/19/2020	11:45	2.5	0.12	0.31	2.75	0.11	0.0755	0.085	0.27	0.235
	6/25/2020	13:00	2.9	0.09	0.27	3.09	0.09	0.0755	0.036	0.13	0.415
	8/12/2020	12:47	3.0	0.10	0.30	3.20	0.10	0.0755	0.071	0.23	0.246
	10/28/2020	9:45	3.0	0.13	0.39	3.26	0.12	0.0755	0.089	0.23	0.290
	8/4/2021	10:37	2.8	0.08	0.23	2.96	0.08	0.0755	0.028	0.12	0.407
	10/22/2021	11:00	4.2	0.20	0.82	4.59	0.18	0.0755	0.460	0.56	0.155
	10/15/2022	11:14	4.0	0.12	0.48	4.24	0.11	0.0755	0.192	0.40	0.161
	7/16/2023	10:55	4.0	0.17	0.68	4.34	0.16	0.0755	0.344	0.51	0.156
		Mean	3.3	0.13	0.43	3.55	0.12	0.0755	0.163	0.31	**0.258**
ws30	5/19/2020	12:55	5.6	0.18	0.99	5.95	0.17	0.0368	0.249	0.25	0.231
	6/25/2020	13:30	3.0	0.13	0.38	3.25	0.12	0.0368	0.054	0.14	0.316
	8/12/2020	12:47	5.7	0.16	0.93	6.03	0.15	0.0368	0.077	0.08	0.668
	10/28/2020	10:20	6.0	0.14	0.83	6.28	0.13	0.0368	0.190	0.23	0.218
	8/4/2021	11:05	4.8	0.12	0.57	5.04	0.11	0.0368	0.071	0.13	0.355
	10/22/2021	11:30	6.0	0.23	1.40	6.47	0.22	0.0368	0.704	0.50	0.137
		Mean	5.2	0.16	0.85	5.50	0.15	0.0368	0.224	0.22	**0.321**
ws31	10/28/2020	9:15	2.0	0.16	0.31	2.31	0.14	0.0915	0.074	0.24	0.335
	8/4/2021	11:32	1.8	0.19	0.34	2.17	0.15	0.0915	0.020	0.06	1.440
	10/22/2021	12:40	2.5	0.26	0.64	3.01	0.21	0.0915	0.270	0.42	0.255
	10/15/2022	10:20	2.4	0.23	0.55	2.86	0.19	0.0915	0.160	0.29	0.348
	7/16/2023	11:30	4.0	0.19	0.76	4.38	0.17	0.0915	0.294	0.38	0.246
		Mean	2.5	0.20	0.52	2.95	0.17	0.0915	0.164	0.28	**0.525**
ws32	6/3/2020	9:50	7.5	0.23	1.69	7.95	0.21	0.0485	1.735	1.03	0.077
	6/25/2020	9:35	8.0	0.18	1.45	8.36	0.17	0.0485	0.835	0.57	0.119
	8/13/2020	15:10	3.2	0.25	0.81	3.71	0.22	0.0485	0.395	0.49	0.163
	10/28/2020	12:00	4.0	0.22	0.89	4.45	0.20	0.0485	0.498	0.56	0.136
	8/4/2021	14:30	5.3	0.15	0.80	5.55	0.14	0.0485	0.373	0.47	0.129
	10/22/2021	15:10	8.7	0.22	1.95	9.15	0.21	0.0485	1.267	0.65	0.121
	5/31/2022	12:30	6.5	0.32	2.07	7.14	0.29	0.0485	2.511	1.21	0.080
	9/14/2022	15:38	7.8	0.17	1.29	8.13	0.16	0.0485	0.620	0.48	0.135
	7/16/2023	9:07	8.4	0.19	1.59	8.78	0.18	0.0485	1.099	0.69	0.102
		Mean	6.6	0.21	1.39	7.02	0.20	0.0485	1.037	0.68	**0.118**
ws33	6/3/2020	13:30	9.9	0.07	0.66	10.03	0.07	0.0590	0.827	1.25	0.032
	6/25/2020	14:00	9.7	0.04	0.42	9.79	0.04	0.0590	0.236	0.56	0.053
	8/11/2020	15:05	10.0	0.05	0.51	10.10	0.05	0.0590	0.127	0.25	0.134
	10/28/2020	8:35	8.5	0.12	1.02	8.74	0.12	0.0590	0.284	0.28	0.208
	8/4/2021	12:05	8.8	0.04	0.37	8.88	0.04	0.0590	0.127	0.34	0.085
	10/22/2021	13:40	7.0	0.20	1.41	7.40	0.19	0.0590	0.699	0.49	0.163
	5/31/2022	13:37	9.0	0.11	0.97	9.22	0.11	0.0590	0.927	0.95	0.057
	10/15/2022	9:15	9.8	0.06	0.58	9.92	0.06	0.0590	0.379	0.66	0.056
	7/26/2023	10:06	9.7	0.06	0.62	9.83	0.06	0.0590	0.433	0.70	0.055
		Mean	9.2	0.08	0.73	9.32	0.08	0.0590	0.449	0.61	**0.094**

Table S2. Runoff characteristics for each watershed. Each variable represents the

Watershed	Years sampled	Samples	Annual discharge (mm)
ws1	2018-2024	7	938.5
ws2	2018-2024	7	-
ws3	2018-2024	7	-
ws4	2018-2023	6	-
ws5	2018-2024	7	2677.1
ws6	2018-2020	3	676.5
ws7	2019-2023	5	1431.7
ws8	2019-2024	6	963.3
ws9	2019-2024	6	1058.3
ws10	2019-2021	3	634.0
ws11	2021-2023	3	1503.4
ws12	2018-2024	7	-
ws13	2018-2023	6	1921.9
ws14	2018-2024	7	727.7
ws15	2018-2019, 2021-2024	6	1296.5
ws16	2021-2024	4	-
ws17	2019-2021, 2023-2024	5	502.6
ws18	2019-2020	2	-
ws19	2021-2024	4	536.4
ws20	2019-2024	6	454.2
ws21	2019-2020	2	-
ws22	2019-2021	3	634.4
ws23	2019-2022	4	1518.4
ws24	2020-2024	5	683.9
ws25	2021-2024	4	1310.8
ws26	2021-2024	4	1034.1
ws27	2020-2023	4	1207.5
ws28	2021-2023	3	417.8
ws29	2021-2024	4	836.3
ws30	2021	1	-
ws31	2021-2024	4	938.0
ws32	2021-2024	4	1070.0
ws33	2021-2024	4	1475.3

mean value. Annual values were calculated using only years in which hydrographs were available fo

Annual Precipitation (mm)	Annual runoff ratio	Total discharge (mm)	Qq (mm)
1312.2	0.72	283.1	150.9
-	-	169.8	99.1
-	-	111.7	67.0
-	-	219.7	129.3
1201.7	2.32	432.4	66.3
1174.1	0.57	164.0	80.0
1240.7	1.21	414.6	186.5
1243.6	0.77	263.1	89.0
1067.0	1.02	389.6	245.6
1127.2	0.60	215.9	124.2
1387.9	1.08	321.9	219.7
-	-	180.0	91.9
1214.3	1.60	452.4	278.1
1273.6	0.57	336.8	303.5
1612.7	0.79	414.2	280.3
-	-	584.2	411.9
1008.1	0.50	220.3	176.8
-	-	346.2	282.6
1233.7	0.43	227.0	169.5
1070.8	0.42	191.5	141.2
-	-	120.7	70.1
1079.4	0.59	170.2	58.2
1115.2	1.33	515.9	276.2
1232.2	0.56	262.9	213.1
1287.9	1.02	527.7	348.4
1224.3	0.85	257.1	86.8
1138.7	1.07	436.9	232.4
1442.0	0.29	194.0	129.4
1613.6	0.52	351.3	280.5
-	-	372.0	255.0
1586.8	0.59	369.7	227.2
1494.7	0.71	502.5	396.4
1550.9	0.95	527.9	282.1

r more than 90% of the days.

Qd (mm)
132.2
70.7
44.7
90.4
366.1
84.0
228.1
174.1
144.0
91.7
102.3
88.1
174.3
33.3
133.9
172.3
59.8
63.6
57.5
50.3
50.7
112.0
239.8
49.7
179.3
170.3
204.5
64.6
70.8
117.0
142.5
106.1
245.7

Table S3. Model selection.

Response	Rank	Intercept	SFW[a]	GP[b]	cumTAZ[c]	Vol[d]	relief[e]	aveCG[f]
$\mathrm{Log}_{10}(Qq)$	1	2.1750	0.0639	0.1067	0	0	0	0.0936
	2	2.1750	0.0638	0.0968	-0.0260	0	0	0.0907
	3	2.1750	0.0656	0.1071	0	0	0	0.0844
	4	2.1750	0.0655	0.0969	-0.0266	0	0	0.0810
	5	2.1728	0.0652	0.1058	0	-0.0363	0	0.0769
	6	2.1758	0.0665	0.0956	-0.0312	0	-0.0395	0.1040
	7	2.1726	0.0652	0.0954	-0.0270	-0.0396	0	0.0724
	8	2.1737	0.0666	0.1062	0	0	0	0.0849
	9	2.1755	0.0655	0.1072	0	0	-0.0242	0.1022
$\mathrm{Log}_{10}(Qd)$	1	2.0069	0.0402	0.0548	-0.0313	0.1483	0.1246	0
	2	2.0067	0.0389	0.0665	0	0.1547	0.1402	0
	3	2.0079	0.0354	0.0543	-0.0339	0.1142	0.1202	0
	4	2.0068	0.0355	0.0549	-0.0335	0.1242	0.1256	0
	5	2.0076	0.0337	0.0670	0	0.1190	0.1368	0
	6	2.0065	0.0340	0.0675	0	0.1287	0.1417	0
	7	2.0058	0.0392	0.0554	-0.0314	0.1537	0.1299	0
	8	2.0055	0.0380	0.0671	0	0.1601	0.1453	0
	9	2.0072	0.0387	0.0666	0	0.1627	0.1434	0

[a] Snowfall water equivalent (mm), [b] Spring precipitation (mm), [c] Positive temperature sums (°C), [d] V

DD[g]	NWNE[h]	Zyou[i]	GP*Vol[j]	SFW*Vol[k]	df	logLik	AICc	delta	weight
0	0	0	0	0	6	45.668	-78.760	0	0.0445
0	0	0	0	0	7	46.576	-78.380	0.380	0.0368
-0.0436	0	0	0	0	7	46.453	-78.133	0.627	0.0325
-0.0455	0	0	0	0	8	47.416	-77.832	0.928	0.0279
0	0	0	0	0	7	46.129	-77.486	1.274	0.0235
0	0	0	0	0	8	47.132	-77.264	1.497	0.0210
0	0	0	0	0	8	47.113	-77.226	1.534	0.0206
0	0.0258	0	0	0	7	45.924	-77.075	1.685	0.0191
0	0	0	0	0	7	45.894	-77.016	1.745	0.0186
0.0578	0.0613	0	0	0.0452	11	46.757	-69.642	0	0.0479
0.0573	0.0649	0	0	0.0437	10	45.592	-69.634	0.008	0.0477
0.0497	0	0	0	0.0415	10	45.334	-69.119	0.523	0.0369
0	0	0	0	0.0376	9	44.094	-68.929	0.713	0.0335
0.0485	0	0	0	0.0394	9	43.969	-68.680	0.963	0.0296
0	0	0	0	0.0355	8	42.780	-68.560	1.082	0.0279
0	0.0505	0	0	0.0396	10	44.991	-68.434	1.209	0.0262
0	0.0542	0	0	0.0379	9	43.832	-68.406	1.236	0.0258
0.0588	0.0647	-0.0185	0	0.0474	11	45.771	-67.670	1.973	0.0179

Volcanic rock proportion (%), [e] Watershed relief (m), [f] Average channel gradient (°), [g] Drainage density (m/k

m^2), [h] North facing proportion (%), [i] Evergreen proportion (%), [j] Volcanic × Spring precipitation, [k] Volcani

ic × Snowfall water equivalent

Table S4. Best model.

Response	Covariate	Standardized coefficien	Std. Error
$Log_{10}(Qq)$	Intercept	2.175	0.0331
	Snowfall water equivalent (mm)	0.064	0.0192
	Spring precipitation (mm)	0.107	0.0133
	Average channel gradient (°)	0.094	0.0326
$Log_{10}(Qd)$	Intercept	2.007	0.0277
	Snowfall water equivalent (mm)	0.040	0.0192
	Spring precipitation (mm)	0.055	0.0158
	Positive temperature sums (℃)	-0.031	0.0203
	Volcanic rock proportion (%)	0.148	0.0353
	Watershed relief (m)	0.125	0.0309
	Drainage density (m km^{-2})	0.058	0.0296
	North facing proportion (%)	0.061	0.0352
	Volcanic × Snowfall water equivalent	0.045	0.0188

Adjusted SE	95%CI	z	p
32.268	2.108 to 2.242	65.692	< 0.001
151.943	0.026 to 0.102	3.332	< 0.01
129.800	0.080 to 0.133	8.007	< 0.001
36.206	0.028 to 0.159	2.875	< 0.01
32.576	1.951 to 2.063	72.480	< 0.001
151.724	0.002 to 0.078	2.092	< 0.05
137.591	0.024 to 0.086	3.480	< 0.001
149.199	-0.071 to 0.009	-1.539	n.s.
33.891	0.077 to 0.220	4.203	< 0.001
43.473	0.062 to 0.186	4.037	< 0.001
32.259	-0.003 to 0.117	1.952	n.s.
33.952	-0.011 to 0.132	1.738	n.s.
149.252	0.007 to 0.083	2.405	< 0.05

Text S
Click here to access/download;attachment to manuscript;Text_SI.docx

Text S1 Data collection of streamflow time-series data

Streamflow time-series data was collected following procedures. First, water depth was observed using an absolute-pressure water-level sensor (U20L-04; HOBO), at sites with gentle channel gradients (< 7°), assuming minimal microtopographic changes and bed conditions considered relatively stable throughout the year. To avoid impacts from gravel collisions while ensuring persistent flow, sensors were placed inside a perforated plastic casing and installed behind cobbles with diameters of several tens of centimeters or behind protruding tree roots along the banks (e.g., structures similar to under-cut banks formed by roots). The plastic casing was fixed to the bed by driving an iron stake (approximately 1 cm in diameter and 1 m in length) into the bed to a depth of about 0.8 m, and attaching the casing to the stake with wires or cable ties. To prevent vertical movement of the sensor inside the casing, a mesh of cable ties was wrapped around the lower end of the casing, and the upper end was secured by connecting the holes in the sensor cap and the casing with cable ties. Observed absolute pressure data were corrected for barometric pressure using HOBOware Pro software ver. 3.7.28 and then calibrated against water depth measured in the field. Barometric pressure data for correction were collected using a same model of sensor installed at a representative elevation within the study area. All data were recorded at 1-hour intervals from 2018 to 2024, although the start year varied among sites, resulting in observation periods of 1 to 7 years depending on watersheds (Table S2).

Second, the conversion from the recorded water-depth data to discharge was performed on the basis of Manning's equation, which is expressed as follows (Hessel et al., 2003):

$$U = \frac{1}{n} R^{\frac{2}{3}} S^{\frac{1}{2}} \quad (1)$$

$$Q = \frac{1}{n} A R^{\frac{2}{3}} S^{\frac{1}{2}} \quad (2)$$

where, U is the flow velocity (m s^{-1}), n is the Manning's roughness coefficient, R is the hydraulic radius (m), and S is the water surface slope (m m^{-1}). By multiplying U by A, the cross-sectional area of the flow, the instantaneous discharge Q (m^3 s^{-1}) is then calculated using Equation (2). Thus, assuming that the water surface slope S remains constant, the temporal variation in discharge $Q(t)$ is expressed as follows:

$$Q(t) = \frac{1}{n} A(t) R(t)^{\frac{2}{3}} S^{\frac{1}{2}} \quad (3)$$

Therefore, obtaining continuous discharge data requires estimating the site-specific Manning's roughness coefficient n, as well as the temporal variations in the cross-sectional area $A(t)$ and the hydraulic radius $R(t)$.

The mean values of the Manning's roughness coefficient n at each watershed were estimated by applying Equation (1) and determining all other parameters (U, A, R, and S) from field measurements

and GIS analysis. For obtaining U, A, R, field measurements were conducted 1-3 times per year at each site during 2020-2023 (4-9 measurements in total). Across the channel as close as possible to the absolute-pressure sensors, flow velocity (electromagnetic current meter VE30; accuracy ±2 cm s^{-1}; 5-second averages at 0.6-depth) and water depth (staff gauge) were recorded at 30-50 cm intervals, from which the mean flow velocity (U) was calculated. The cross-sectional area A was simply determined by approximating the channel cross-section as a rectangle and calculating wetted surface width (m), W and water depth (m), D (i.e., $W \times D$), where D was given as the mean measured depth at the discharge-measurement site. The hydraulic radius R was defined as A divided by the wetted perimeter (m), P, and under the rectangular-section assumption, P was expressed as $W+2D$. The water surface slope S was obtained as the mean channel gradient over a total distance of 200 m (100 m upstream and 100 m downstream from the observation site), calculated using the 5-m DEM of the Geospatial Information Authority of Japan in ArcGIS Pro ver. 3.1.0. The mean values of the estimated n were then applied to calculate continuous water discharge using Equation (3). In Equation 3, temporal variations in the cross-sectional area $A(t)$ and hydraulic radius $R(t)$ were calculated from changes in the wetted cross-sectional geometry associated with changes in water depth, based on field surveys. Cross-sectional surveys were conducted at each site in October-November of the first observation year using a rotating laser level (RL-H5A, TOPCON). Level measurements were recorded at 0.1-1.0 m intervals, depending on channel bed topography. The calculating hourly instantaneous discharge data ($m^3\ s^{-1}\ h^{-1}$) were then converted to daily cumulative discharge ($m^3\ day^{-1}\ day^{-1}$) and used for analyzing snowmelt runoff characteristics.

Text S2 Calculation of annual precipitation for each watershed

Annual precipitation used to calculate the annual runoff ratio was obtained from the Agro-Meteorological Grid Square Data provided by the National Agriculture and Food Research Organization (Ohno et al., 2016). This dataset provides daily precipitation (Code: APCP) at a 1-km spatial resolution. The Sorachi River basin was divided into 1-km grid cells, and daily precipitation data were extracted for the centroid of each grid cell within each watershed. Watershed-mean daily precipitation was then calculated by averaging the values of all grid cells within each watershed. Annual precipitation was obtained by summing the watershed-mean daily precipitation over each year.

REFERENCES

Hessel R, Jetten VG, Zhang G (2003) Estimating Manning's n for steep slopes. Catena 54:77–91. https://doi.org/10.1016/S0341-8162(03)00058-4

Ohno H, Sasaki K, Ohara G, Nakazono K (2016) Development of grid square air temperature and precipitation data compiled from observed, forecasted, and climatic normal data. Climate in Biosphere 16:71–79. https://doi.org/10.2480/cib.J-16-028